



138
344
THS

2004

60052231

This is to certify that the
thesis entitled

REGULATION OF NONLINEAR SYSTEMS USING
CONDITIONAL INTEGRATORS

presented by

Abhyudai Singh

has been accepted towards fulfillment
of the requirements for the

M.S. degree in Electrical Engineering

Hassan Khalid
Major Professor's Signature

8/24/2004

Date

LIBRARY
Michigan State
University

PLACE IN RETURN BOX to remove this checkout from your record.
TO AVOID FINES return on or before date due.
MAY BE RECALLED with earlier due date if requested.

DATE DUE	DATE DUE	DATE DUE

REGULATION OF NONLINEAR SYSTEMS USING
CONDITIONAL INTEGRATORS

By

Abhyudai Singh

A THESIS

Submitted to
Michigan State University
in partial fulfillment of the requirements
for the degree of

MASTER OF SCIENCE

Department of Electrical Engineering

2004

ABSTRACT

REGULATION OF NONLINEAR SYSTEMS USING
CONDITIONAL INTEGRATORS

By
Abhyudai Singh

Regulation of nonlinear systems using conditional integrators is studied. Previous work introduced the tool of conditional integrators that provide integral action inside a boundary layer while acting as stable systems outside, leading to improvement in transient response while achieving asymptotic regulation in the presence of unknown constant disturbances or parameter uncertainties. The approach, however, is restricted to a sliding mode control framework. This thesis extends this tool to a fairly general class of state feedback control laws, with the stipulation that we know a Lyapunov function for the closed-loop system. Asymptotic regulation with improvement in transient response is done by using the Lyapunov redesign technique to implement the state feedback control as a saturated high-gain feedback and introducing a conditional integrator to provide integral action inside a boundary layer. Improvement in the transient response using conditional integrators is demonstrated with an experimental application to the Pendubot.

To my family

ACKNOWLEDGMENTS

I would like to express my deepest appreciation to the following people:

To my advisor Dr. Hassan K. Khalil for his guidance and insight. It has been my pleasure, and indeed privilege to have worked with him. His pure, unselfish and honest passion for the subject will always serve as an example and inspiration for me.

To my grandparents (V. K. S. Chaudhary, G. B. Singh and K. D. Singh), who instilled in me an appreciation for honesty and hardwork.

And to my parents (Yatindra and Neeta Singh), who have supported me, encouraged me, and believed in me.

TABLE OF CONTENTS

LIST OF FIGURES	vii
1 Introduction	1
2 Regulation using Conditional Integrators	4
2.1 Problem Statement and Controller design	4
2.2 Class of Systems	8
2.3 Asymptotic Regulation	14
2.4 Performance	23
3 Output Feedback of Minimum-Phase Systems	32
3.1 Problem Statement	32
3.2 Partial State Feedback Design	36
3.3 Output Feedback Design	37
3.4 Comparison of Controllers	42
4 Application to the Pendubot	47
4.1 The Pendubot	47
4.2 Mathematical Model	49
4.3 The Equilibrium Manifold	51
4.4 Controlling The Pendubot	52
4.5 Hardware Description	56

4.6	Observer design	56
4.7	Addition of Uncertainty	57
4.8	Integral action	59
4.9	Conditional Integrators	59
5	Conclusion	62
	APPENDICES	64
A	Controller Design	64
	A.1 Linear Controller	64
	A.2 Traditional Integral Action	65
	A.3 Conditional Integrator	66
	BIBLIOGRAPHY	67

LIST OF FIGURES

2.1	Two-link robot.	11
2.2	Plot of error $\ x_1(t) - x_1^*(t)\ $ for systems (2.38) and (2.39) with $\mu = 1$ (solid), $\mu = .1$ (dashed) and plot of $s = \ y + \sigma\ $ (dashed) for $\mu = 1$, with initial conditions $x_1(0) = x_1^*(0) = 0, x_2(0) = x_2^*(0) = -20$ and $\sigma(0) = 0$	30
2.3	Plot of error $\ x_1(t) - x_1^*(t)\ $ for systems (2.40) and (2.41) with $\mu = 1$ (solid), $\mu = .1$ (dashed) and plot of $s = \ y + \sigma\ $ (dashed) for $\mu = 1$, with initial conditions $x_1(0) = x_1^*(0) = 0, x_2(0) = x_2^*(0) = -15$ and $\sigma(0) = 0$	31
3.1	Plots of $x_1(t), x_2(t)$ and $x_3(t)$ for the controller design (3.20) (dashed) and the controller design using sliding mode control (solid)	45
3.2	Plots of $u_1(t)$ and $u_2(t)$ for the controller design (3.20) (dashed) and the controller design using sliding mode control (solid)	46
4.1	Front and side view drawing of the Pendubot.	48
4.2	The pendubot arm at a: Controllable position, b: Uncontrollable position	53
4.3	Trajectories for angle q_1 for different balancing controls, linear controller with no disturbance (solid), linear controller with constant disturbance of 1.6V in the control (dotted), linear state feedback integral controller with constant disturbance of 1.6V in the control (dashed) .	58
4.4	Trajectories for angles q_1 for different balancing controls with disturbance of 1.6V in the control, traditional integral action (solid), conditional integrator with $\mu=0.25$ (dashed), conditional integrator with $\mu=0.15$ (dotted)	60

4.5 Trajectories for angles q_2 for different balancing controls with disturbance of $1.6V$ in the control, traditional integral action (solid), conditional integrator with $\mu=0.25$ (dashed), conditional integrator with $\mu=0.15$ (dotted) 61

CHAPTER 1

Introduction

When a system is subjected to unknown constant disturbances or parameter uncertainties that cause a shift in the equilibrium point, we need to use integral action to achieve robust asymptotic regulation. The traditional approach for introducing integral action is to augment integrators with the system and design feedback control to stabilize the augmented system [4], [7], [8], [9], [10], [12]. The integrators are introduced in such a way that they create an equilibrium point at which the regulation error is zero. Hence, stabilizing the equilibrium point ensures asymptotic regulation. In this approach, achieving asymptotic regulation usually happens at the expense of degrading the transient response. A new approach of conditional integrators has been recently introduced in [14]. The work [14] deals with continuous implementation of sliding mode control and introduces conditional integrators that provide integral action inside a boundary layer of the sliding surface, while acting like a stable system outside it. The striking feature of the results of [14] is that the state of the conditional integrator is always of the order of μ (the width of the boundary layer) and as $\mu \rightarrow 0$ the trajectories of the closed-loop system approach the

trajectories obtained under ideal sliding mode control without integral action, which provides analytical confirmation of the property that integral action is introduced without degrading the transient response.

In this thesis we extend the tool of conditional integrators beyond the sliding mode control framework. Towards that end, we consider a stabilizing, locally Lipschitz, state feedback control law that stabilizes the origin of a nonlinear system and assume that we know a Lyapunov function for the closed-loop system. Then, we perturb the system with a matched uncertainty that causes a shift in the equilibrium point. To recover asymptotic regulation of the state, we introduce integral action via a conditional integrator. The key idea is to use Lyapunov redesign to implement the state feedback control as a saturated high-gain feedback and then introduce the conditional integrator to provide integral action inside a boundary layer. We prove analytically that, for sufficiently small μ , conditional integrators can recover asymptotic regulation of the state to the origin in the presence of matched uncertainty and, under certain assumptions, global asymptotic regulation can be achieved.

We also show that, for a certain compact set of the initial states, as the width of the boundary layer approaches zero, trajectories of the system with conditional integrator approach those of a system with no integral action. Hence, degradation in transient response due to integral action can be attenuated by tuning the width of the boundary layer without sacrificing asymptotic regulation. In the afore-mentioned

results the goal is to regulate the state of the system to zero despite the constant disturbance or parameter uncertainty. In many regulation problems, however, such requirements could be restrictive and it might be sufficient to regulate the states to a disturbance-dependent equilibrium point at which the regulation error is zero. In Chapter 3, we consider such regulation for a class of minimum-phase, input-output linearizable, nonlinear systems which is basically the same class studied in [14], aside from some differences in the technical assumptions. As in [14], we study output feedback control using high-gain observers, but, unlike [14], we do not use sliding mode control. Instead, we use a saturated high-gain feedback implementation of the linearizing feedback control.

Finally, in Chapter 4, we demonstrate the improvement in transient response with conditional integrators by an application to the Pendubot.

CHAPTER 2

Regulation using Conditional Integrators

2.1 Problem Statement and Controller design

Consider a nonlinear system represented by

$$\dot{x} = f(x) + G(x)u \quad (2.1)$$

where $u \in R^m$ is the control input, $x \in R^n$ is the state vector, $G(x), f(x)$ are, possibly unknown, sufficiently smooth functions in a domain $\mathcal{X} \subset R^n$, with $\{0\} \in \mathcal{X}$, and $f(0) = 0$. Suppose there are, possibly unknown, locally Lipschitz function $\psi(x)$, with $\psi(0) = 0$, and C^2 Lyapunov function $V(x)$, with $\frac{\partial V}{\partial x}(0) = 0$, such that the following assumptions are satisfied.

Assumption 1:

$$\frac{\partial V}{\partial x}[f(x) + G(x)\psi(x)] \leq -W(x), \quad \forall x \in \mathcal{X} \quad (2.2)$$

for some continuous positive definite function $W(x)$.

Assumption 2: $\frac{\partial V}{\partial x}G(x)$ can be expressed as $\frac{\partial V}{\partial x}G(x) = h^T(x)L(x)$ where $h(x)$ is a known continuous function with $h(0) = 0$ and $L(x)$ is a, possibly unknown, continuous function satisfying $L^T(x) + L(x) \geq 2\lambda I$ and* $\|L(x)\| \leq k$, $\forall x \in \mathcal{X}$ where $k \geq \lambda > 0$.

Assumption 3: The square matrix $M(x) = \frac{\partial h}{\partial x}G(x)$ has the property that $M(0) + M^T(0)$ is positive definite.

Let $\Omega = \{V(x) \leq c_1\} \subset \mathcal{X}$ be a compact set and

$$\lambda_p = \lambda_{\min} \left\{ \frac{[M(0) + M^T(0)]}{2} \right\}, \quad k_p = \|M(0)\| \quad (2.3)$$

where $\lambda_{\min}\{\cdot\}$ stands for the smallest eigenvalue of a positive definite matrix. Suppose system (2.1) is perturbed by a sufficiently smooth matched uncertainty $\delta(x)$ that causes a shift in the equilibrium point, i.e, $\delta(0) \neq 0$. The perturbed system can be

* $\|\cdot\| = \|\cdot\|_2$

written as

$$\begin{aligned}\dot{x} &= f(x) + G(x)[u + \delta(x)] \\ &= f(x) + G(x)\psi(x) + G(x)u + G(x)[\delta(x) - \psi(x)].\end{aligned}\tag{2.4}$$

Let $\beta(x) \geq 0$ be a known continuous function such that

$$\|\delta(x) - \psi(x)\| \leq \beta(x), \quad \forall x \in \Omega.$$

Choose a locally Lipschitz function $\alpha(x)$ such that, $\forall x \in \Omega$,

$$\alpha(x) \geq k_\alpha \beta(x) + \alpha_0,\tag{2.5}$$

where $k_\alpha = \max\left\{\frac{k}{\lambda}, \frac{k_p}{\lambda_p}\right\} \geq 1$ and $\alpha_0 > 0$. We make the following local assumption on the functions $G(x)$, $f(x)$, $\delta(x)$, $h(x)$, $\psi(x)$ and $\alpha(x)$.

Assumption 4: There exist non-negative constants k_1 to k_6 such that

$$\begin{aligned}\|\delta(x) - \delta(0) - \psi(x)\| &\leq k_1 \|h(x)\| + k_2 \sqrt{W(x)} \\ \left\| \frac{\partial h}{\partial x} [f(x) + G(x)\psi(x)] \right\| &\leq k_3 \|h(x)\| + k_4 \sqrt{W(x)} \\ \|\alpha(x) - \alpha(0)\| &\leq k_5 \|h(x)\| + k_6 \sqrt{W(x)}\end{aligned}$$

in some neighborhood of $x = 0$.

If $W(x) \geq k_w \|x\|^2, k_w > 0$, near the origin, then any locally Lipschitz function can be bounded by $k_a \sqrt{W(x)}$ for some $k_a > 0$. Define the vector saturation function $\varphi(y)$ by

$$\varphi(y) = \begin{cases} \frac{y}{\|y\|} & \text{if } \|y\| \geq 1 \\ y & \text{if } \|y\| \leq 1. \end{cases} \quad (2.6)$$

It is not hard to verify that the saturated high-gain feedback control

$$u = -\alpha(x)\varphi\left(\frac{y}{\mu}\right), \quad \mu > 0, \quad (2.7)$$

where $y = h(x)$, achieves practical stabilization in the sense that, within a finite time interval, $x(t)$ reaches a neighborhood of the origin whose size is a class \mathcal{K} function of μ . Hence, by reducing μ , we can reduce the ultimate bound on x . However, in reality, we cannot make the ultimate bound arbitrarily small because it would require μ to be arbitrarily small; hence, inducing chattering, excitation of unmodeled fast dynamics, and other well-known problems. To achieve asymptotic regulation without forcing μ to be arbitrarily small, we introduce a conditional integrator by modifying (2.7) to

$$u = -\alpha(x)\varphi\left(\frac{y + \gamma\sigma}{\mu}\right), \quad (2.8)$$

where σ is the output of the conditional integrator

$$\dot{\sigma} = -\gamma\sigma + \mu\varphi\left(\frac{y + \gamma\sigma}{\mu}\right), \quad \gamma > 0. \quad (2.9)$$

Because $\|\varphi(y)\| \leq 1$, $\forall y \in R^m$, it can be verified that $\|\sigma(t)\| \leq \mu/\gamma$ for all $t \geq 0$ provided $\|\sigma(0)\| \leq \mu/\gamma$, as from (2.9)

$$\begin{aligned}\sigma^T \dot{\sigma} &= -\gamma \sigma^T \sigma + \mu \sigma^T \varphi \left(\frac{y + \gamma \sigma}{\mu} \right) \\ &\leq -\gamma \|\sigma\|^2 + \mu \|\sigma\| \leq 0, \quad \forall \|\sigma\| \geq \frac{\mu}{\gamma}.\end{aligned}\tag{2.10}$$

Inside the boundary layer $\{\|y + \gamma \sigma\| \leq \mu\}$, (2.9) reduces to

$$\dot{\sigma} = -\gamma \sigma + \mu \left(\frac{y + \gamma \sigma}{\mu} \right) = y,\tag{2.11}$$

which provides integral action.

2.2 Class of Systems

We will now show that Assumptions 1-4 are satisfied for a class of feedback linearizable systems. Consider the system

$$\begin{aligned}\dot{\xi}_1^i &= \xi_2^i \\ &\vdots \\ \dot{\xi}_{ri-1}^i &= \xi_{ri}^i \\ \dot{\xi}_{ri}^i &= b_i(\xi, \theta) + \sum_{j=1}^m d_{ij}(\xi, \theta) u_j, \quad 1 \leq i \leq m \\ y_i &= \xi_1^i,\end{aligned}\tag{2.12}$$

where $u = [u_1, \dots, u_m]^T \in \mathcal{U} \in R^m$ is the control input, $\xi = [\xi_1^1, \dots, \xi_{r_1}^1, \dots, \xi_1^m, \dots, \xi_{r_m}^m]^T \in \mathcal{X} \in R^n$ is the state vector, with $\{0\} \in \mathcal{X}$, $\theta \in \Theta \in R^w$ is a vector of unknown constant parameters, and the functions $b_i(\xi, \theta)$ and $d_{i,j}(\xi, \theta)$ are locally Lipschitz in their arguments over the domain of interest, with $b_i(0, \theta) = 0, \forall \theta \in \Theta$. We assume that the decoupling matrix $D(\xi, \theta) = \{d_{ij}(\xi, \theta), 1 \leq i \leq m, 1 \leq j \leq m\}$ is nonsingular $\forall \xi \in \mathcal{X}$ and $\forall \theta \in \Theta$. System (2.12) can be written as

$$\begin{aligned} \dot{\xi} &= A\xi + B[b(\xi, \theta) + D(\xi, \theta)u] \\ &= A\xi + B[b(\xi, \theta) + D(\xi, \hat{\theta})D^{-1}(\xi, \hat{\theta})D(\xi, \theta)u], \end{aligned}$$

where

$$A = \text{block diag}[A_1, \dots, A_m], \quad (2.13)$$

$$A_i = \begin{bmatrix} 0 & 1 & \dots & \dots & 0 \\ 0 & 0 & 1 & \dots & 0 \\ \vdots & & & & \vdots \\ 0 & \dots & \dots & 0 & 1 \\ 0 & \dots & \dots & \dots & 0 \end{bmatrix}_{r_i \times r_i},$$

$$B = \text{block diag}[B_1, \dots, B_m], \quad B_i = \begin{bmatrix} 0 \\ 0 \\ \vdots \\ 0 \\ 1 \end{bmatrix}_{r_i \times 1}, \quad (2.14)$$

$$b(\xi, \theta) = \begin{bmatrix} b_1(\xi, \theta) \\ \vdots \\ b_m(\xi, \theta) \end{bmatrix},$$

$1 \leq i \leq m$, and $\hat{\theta}$ is a nominal value of θ . It can be seen that Assumption 1 is satisfied with

$$\psi(\xi, \theta) = D^{-1}(\xi, \theta)[-b(\xi, \theta) - K\xi], \quad V(\xi) = \xi^T P \xi, \quad W(\xi) = -\xi^T \xi,$$

where the matrix K is chosen such that $A - BK$ is Hurwitz and $P = P^T$ is the solution of the Lyapunov equation $P(A - BK) + (A - BK)^T P = -I$. As $D^{-1}(\xi, \hat{\theta})D(\xi, \theta) = I$ for $\theta = \hat{\theta}$ it must be true that for some perturbation of θ around $\hat{\theta}$,

$$\frac{[D^{-1}(\xi, \hat{\theta})D(\xi, \theta)] + [D^{-1}(\xi, \hat{\theta})D(\xi, \theta)]^T}{2} > 0. \quad (2.15)$$

Let (2.15) be satisfied for $\theta \in \Theta_1 \subset \Theta$. For the single input case, condition (2.15) implies that the scalars $D(\xi, \theta)$ and $D(\xi, \hat{\theta})$ have the same sign. With (2.15), Assumption 2 will be satisfied with $h^T(\xi, \hat{\theta}) = \frac{\partial V(\xi)}{\partial \xi} B D(\xi, \hat{\theta})$ and $L(\xi, \theta) = D^{-1}(\xi, \hat{\theta})D(\xi, \theta)$.

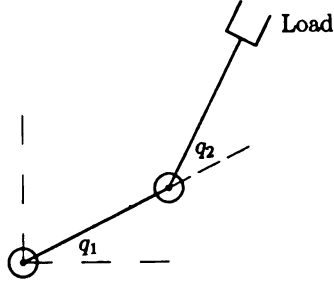


Figure 2.1. Two-link robot.

As $V(\xi)$ is quadratic and $\text{rank}[D(0, \hat{\theta})] = m$

$$D^T(\xi, \hat{\theta})B^T \frac{\partial^2 V(\xi)}{\partial \xi^2} BD(\xi, \hat{\theta}) \Big|_{\xi=0} > 0.$$

Using similar arguments as used for (2.15), it can be shown that there exists a set $\Theta_2 \subset \Theta$ such that the matrix $D_1(\theta, \hat{\theta}) = D^T(\xi, \hat{\theta})B^T \frac{\partial^2 V(\xi)}{\partial \xi^2} BD(\xi, \hat{\theta}) [D^{-1}(\xi, \hat{\theta})D(\xi, \theta)] \Big|_{\xi=0}$ satisfies

$$\frac{D_1(\theta, \hat{\theta}) + D_1^T(\theta, \hat{\theta})}{2} > 0 \quad (2.16)$$

for $\theta \in \Theta_2$. Inequality (2.16) satisfies Assumption 3. Finally, Assumption 4 is also satisfied as $W(\xi)$ is quadratic. Hence, Assumption 1-4 will be satisfied $\forall \theta \in \Theta_1 \cap \Theta_2 \subset \Theta$.

Example : The two-link robot shown in Figure 2.1, can be modeled [13] by the

following equation

$$M(q)\ddot{q} + C(q, \dot{q})\dot{q} + D\dot{q} + g(q) = u,$$

where q is a two-dimensional vector of generalized coordinates representing joint positions, u is a two-dimensional control (torque) input. $M(q)$ is a symmetric inertia matrix, which is positive definite for all $q \in R^2$ and is given by

$$M(q) = \begin{bmatrix} a_1 + 2a_4 \cos q_2 & a_2 + a_4 \cos q_2 \\ a_2 + a_4 \cos q_2 & a_3 \end{bmatrix},$$

where a_1, \dots, a_4 are positive constants. The term $C(q, \dot{q})\dot{q}$ accounts for centrifugal and coriolis forces and is given by

$$C(q, \dot{q})\dot{q} = a_4 \sin q_2 \begin{bmatrix} -\dot{q}_2 & -(\dot{q}_1 + \dot{q}_2) \\ \dot{q}_1 & 0 \end{bmatrix}.$$

The term $D\dot{q}$ accounts for viscous damping, where D is a positive semidefinite matrix. However, in this example we will neglect damping and take $D = 0$. The term $g(q)$, which accounts for the gravity forces, is given by

$$g(q) = \begin{bmatrix} b_1 \cos q_1 + b_2 \cos(q_1 + q_2) \\ b_2 \cos(q_1 + q_2) \end{bmatrix},$$

where b_1 and b_2 are positive constants. These constants a_1, \dots, a_4, b_1 and b_2 depend on masses, moment of inertia, lengths of the two links, acceleration due to gravity

and the load kept on the robot. The nominal values corresponding to no load on the robot are

$$\hat{a}_1 = 200.01, \hat{a}_2 = 23.5, \hat{a}_3 = 122.5, \hat{a}_4 = 25, \hat{b}_1 = 784.8, \hat{b}_2 = 245.25.$$

The state space equation for the two link robot is given by

$$\dot{x} = Ax + B\{\hat{M}^{-1}(q)\hat{M}(q)M^{-1}(q)[u - C(q, \dot{q})\dot{q} - g(q)]\}, \quad x = \begin{bmatrix} q_1 \\ \dot{q}_1 \\ q_2 \\ \dot{q}_2 \end{bmatrix},$$

where A and B given by (2.13) and (2.14) respectively with $\{r_i = 2, 1 \leq i \leq 2\}$ and

$$\hat{M}(q) = \begin{bmatrix} \hat{a}_1 + 2\hat{a}_4 \cos q_2 & \hat{a}_2 + \hat{a}_4 \cos q_2 \\ \hat{a}_2 + \hat{a}_4 \cos q_2 & \hat{a}_3 \end{bmatrix}.$$

It can be seen that Assumption 1 is satisfied with

$$\psi(x) = [C(q, \dot{q})\dot{q} + g(q) - M(q)Kx], \quad V(x) = x^T P x, \quad W(x) = -10x^T x,$$

$$P = \begin{bmatrix} 15.7074 & 0.1548 & -0.4792 & 0.0103 \\ 0.1548 & 0.4273 & 0.0074 & 0.0143 \\ -0.4792 & 0.0074 & 18.4157 & 0.1014 \\ 0.0103 & 0.0143 & 0.01014 & 0.3423 \end{bmatrix},$$

$$K = \begin{bmatrix} 32.492 & 12.0791 & -2.8711 & -0.4700 \\ -2.9927 & -.4903 & 49.5071 & 14.9209 \end{bmatrix}.$$

Due to an unknown load, the actual system parameters are perturbed to

$$a_1 = 259.7, \quad a_2 = 58.19, \quad a_3 = 157.19, \quad a_4 = 56.25, \quad b_1 = 1030.1, \quad b_2 = 551.8125.$$

It can be verified that for this perturbation, $\forall q \in R^2$,

$$\begin{aligned} & [\hat{M}(q)M^{-1}(q)] + [\hat{M}(q)M^{-1}(q)]^T > 0 \\ & [M^{-1T}(q)BPB^T\hat{M}^{-1}(q)] + [M^{-1T}(q)B^T P B \hat{M}^{-1}(q)]^T > 0. \end{aligned}$$

Hence, Assumptions 2 and 3 are satisfied with

$$h^T(x) = 2x^T P B \hat{M}^{-1}(q), \quad L(x) = \hat{M}(q)M^{-1}(q).$$

Finally, Assumption 4 is also satisfied as $W(x)$ is quadratic.

2.3 Asymptotic Regulation

In this section we prove that, for sufficiently small μ , the system (2.4), (2.8), (2.9)

has an asymptotically stable equilibrium point at which $x = 0$.

Theorem 1: Suppose Assumptions 1-4 are satisfied. Then, there exists $\mu^* > 0$ such

that $\forall \mu \in (0, \mu^*]$

a) The system (2.4), (2.8), (2.9) has an asymptotically stable equilibrium point at $(x = 0, \bar{\sigma} = \frac{\mu}{\alpha(0)\gamma}\delta(0))$ and $\Sigma = \{V(x) \leq c_1\} \times \{\|\sigma\| \leq \mu/\gamma\}$ is a subset of the region of attraction.

b) If (2.5) and Assumptions 1, 2 hold globally, $V(x)$ is radially unbounded, and

$$\alpha(x) \leq k_g W(x) + c_g, \quad \forall x \in R^n \quad (2.17)$$

for some $k_g, c_g > 0$, then, $\forall (x(0), \sigma(0)) \in R^n \times \{\|\sigma\| \leq \mu/\gamma\}$, $\lim_{t \rightarrow \infty} x(t) = 0$.

Proof : a) The proof is divided into three parts. First we show that all trajectories of the system (2.4), (2.8), (2.9) starting in the set Σ reach a positively invariant set $\Sigma_\mu = \{V(x) \leq \rho(\mu)\} \times \{\|\sigma\| \leq \mu/\gamma\}$ in finite time, where ρ is a class \mathcal{K} function. Then we show that the trajectories in the set Σ_μ enter the boundary layer $\{\|y + \gamma\sigma\| \leq \mu\}$ in finite time. Inside the boundary layer, we show that the system has an asymptotically stable equilibrium point at which $x = 0$.

To show that all trajectories starting in Σ enter Σ_μ in finite time, we calcu-

late \dot{V} for $(x, \sigma) \in \Sigma$.

$$\begin{aligned}
\dot{V} &= \frac{\partial V}{\partial x}[f(x) + G(x)\psi(x)] + \frac{\partial V}{\partial x}G(x)u + \frac{\partial V}{\partial x}G(x)[\delta(x) - \psi(x)] \\
&\leq -W(x) - y^T \alpha(x)L(x)\varphi\left(\frac{y + \gamma\sigma}{\mu}\right) + y^T L(x)[\delta(x) - \psi(x)] \\
&= -W(x) - (y + \gamma\sigma)^T \alpha(x)L(x)\varphi\left(\frac{y + \gamma\sigma}{\mu}\right) + \alpha(x)\gamma\sigma^T L(x)\varphi\left(\frac{y + \gamma\sigma}{\mu}\right) \\
&\quad - \gamma\sigma^T L(x)[\delta(x) - \psi(x)] + (y + \gamma\sigma)^T L(x)[\delta(x) - \psi(x)].
\end{aligned}$$

If $\|(y + \gamma\sigma)\| \geq \mu$, $\varphi\left(\frac{y + \gamma\sigma}{\mu}\right) = \frac{(y + \gamma\sigma)}{\|(y + \gamma\sigma)\|}$. Using $\gamma\|\sigma\| \leq \mu$, $L^T(x) + L(x) \geq 2\lambda I$, $\|L(x)\| \leq k$ and (2.5) we have

$$\begin{aligned}
\dot{V} &\leq -W(x) - \lambda\alpha(x)\|(y + \gamma\sigma)\| + k\beta(x)\|(y + \gamma\sigma)\| + k[\alpha(x) + \beta(x)]\mu \\
&\leq -W(x) + \alpha_1\mu, \quad \alpha_1 = \max_{x \in \Omega} k[\alpha(x) + \beta(x)].
\end{aligned}$$

If $\|(y + \gamma\sigma)\| \leq \mu$, $\varphi\left(\frac{y + \gamma\sigma}{\mu}\right) = \frac{y + \gamma\sigma}{\mu}$ and

$$\begin{aligned}
\dot{V} &\leq -W(x) + k[\alpha(x) + 2\beta(x)]\mu \tag{2.18} \\
&\leq -W(x) + \alpha_2\mu, \quad \alpha_2 = \max_{x \in \Omega} k[\alpha(x) + 2\beta(x)] \geq \alpha_1.
\end{aligned}$$

Thus, $\forall (x, \sigma) \in \Sigma$, $\dot{V} \leq -W(x) + \alpha_2\mu$. Hence, from ([11], Theorem 4.18), for sufficiently small μ , the set Σ is positively invariant and all trajectories starting in Σ enter a positively invariant set $\Sigma_\mu = \{V(x) \leq \rho(\mu)\} \times \{\|\sigma\| \leq \mu/\gamma\}$ in finite time, where ρ is a class \mathcal{K} function.

Next, we show that the trajectories reach the boundary layer $\{\|y + \gamma\sigma\| \leq \mu\}$ in finite time. For $(x, \sigma) \in \Sigma_\mu$, we have

$$\begin{aligned} \dot{y} &= \frac{\partial h}{\partial x}[f(x) + G(x)\psi(x)] + M(0)[u - \psi(x) + \delta(x)] \\ &\quad + [M(x) - M(0)][u - \psi(x) + \delta(x)]. \end{aligned} \quad (2.19)$$

From (2.8) and (2.9),

$$\begin{aligned} (\dot{y} + \gamma\dot{\sigma}) &= -\alpha(x)M(0)\varphi\left(\frac{y + \gamma\sigma}{\mu}\right) + N(x) + M(0)[\delta(x) - \psi(x)] - \gamma^2\sigma \\ &\quad + \gamma\mu\varphi\left(\frac{y + \gamma\sigma}{\mu}\right), \end{aligned}$$

where

$$N(x) = \frac{\partial h}{\partial x}[f(x) + G(x)\psi(x)] + [M(x) - M(0)][u - \psi(x) + \delta(x)].$$

As we are already inside the set Σ_μ and $N(0) = 0$, $\|N(x) + \gamma\dot{\sigma}\|$ can be bounded by a class \mathcal{K} function $\rho_1(\mu)$, i.e.

$$\left\| N(x) + \gamma\mu\varphi\left(\frac{y + \gamma\sigma}{\mu}\right) - \gamma^2\sigma \right\| \leq \rho_1(\mu).$$

Let $V_1 = \frac{1}{2}\|y + \gamma\sigma\|^2$.

$$\begin{aligned} \dot{V}_1 &= (y + \gamma\sigma)^T(\dot{y} + \gamma\dot{\sigma}) \\ &\leq -\alpha(x)(y + \gamma\sigma)^T M(0)\varphi\left(\frac{y + \gamma\sigma}{\mu}\right) + (y + \gamma\sigma)^T M(0)[\delta(x) - \psi(x)] \end{aligned}$$

$$+\rho_1(\mu)\|(y + \gamma\sigma)\|.$$

If $\|y + \gamma\sigma\| \geq \mu$, $\varphi\left(\frac{y+\gamma\sigma}{\mu}\right) = \frac{(y+\gamma\sigma)}{\|(y+\gamma\sigma)\|}$ and, using (2.3) and (2.5),

$$\begin{aligned} \dot{V}_1 &\leq -\lambda_p \left[\alpha(x) - \frac{k_p}{\lambda_p} \beta(x) - \frac{\rho_1(\mu)}{\lambda_p} \right] \|y + \gamma\sigma\| \\ &\leq -\lambda_p \left[\alpha_o - \frac{\rho_1(\mu)}{\lambda_p} \right] \|(y + \gamma\sigma)\|. \end{aligned}$$

Thus, for sufficiently small μ , all trajectories inside Σ_μ would reach the boundary layer $\{\|y + \gamma\sigma\| \leq \mu\}$ in finite time. Inside the boundary layer, the system (2.4), (2.8), (2.9) is given by

$$\begin{aligned} \dot{x} &= f(x) + G(x)\psi(x) - \alpha(x)G(x) \left(\frac{y + \gamma\sigma}{\mu} \right) + G(x)[\delta(x) - \psi(x)] \\ \dot{\sigma} &= -\gamma\sigma + \mu \left(\frac{y + \gamma\sigma}{\mu} \right) = y. \end{aligned}$$

We can see that $\left(x = 0, \bar{\sigma} = \frac{\mu}{\alpha(0)\gamma}\delta(0)\right)$ is an equilibrium point. Defining $\tilde{\sigma} = \sigma - \bar{\sigma}$ and $\tilde{\delta}(x) = \delta(x) - \delta(0)$, the system inside the boundary layer can be written as

$$\begin{aligned} \dot{x} &= f(x) + G(x)\psi(x) + G(x) \left\{ -\alpha(x) \left(\frac{y + \gamma\tilde{\sigma}}{\mu} \right) - \frac{\delta(0)}{\alpha(0)} [\alpha(x) - \alpha(0)] \right\} \\ &\quad + G(x)[\tilde{\delta}(x) - \psi(x)] \end{aligned} \tag{2.20}$$

$$\dot{\tilde{\sigma}} = y. \tag{2.21}$$

Define the Lyapunov function

$$V_2 = V(x) + \frac{b}{2}\bar{\sigma}^T\bar{\sigma} + \frac{c}{2}(y + \gamma\bar{\sigma})^T(y + \gamma\bar{\sigma}),$$

where b and c are positive constants to be chosen. Calculating \dot{V}_2 along the trajectories of the system (2.20) and (2.21), we obtain

$$\dot{V}_2 = \dot{V} + b\bar{\sigma}^T y + c(y + \gamma\bar{\sigma})^T \left(\frac{\partial h}{\partial x} \dot{x} + \gamma y \right). \quad (2.22)$$

Using Assumptions 1, 2 and 4 yields

$$\begin{aligned} \dot{V} &= \frac{\partial V}{\partial x} [f(x) + G(x)\psi(x)] + y^T L(x) \left\{ -\alpha(x) \left(\frac{y + \gamma\bar{\sigma}}{\mu} \right) - \frac{\delta(0)}{\alpha(0)} [\alpha(x) - \alpha(0)] \right\} \\ &\quad + y^T L(x) [\bar{\delta}(x) - \psi(x)] \\ &\leq -W(x) - \alpha(x) \frac{\lambda}{\mu} \|y\|^2 - \alpha(x) y^T L(x) \gamma \frac{\bar{\sigma}}{\mu} + k_7 \|y\|^2 + k_8 \|y\| \sqrt{W(x)} \end{aligned}$$

for some non-negative constants k_7, k_8 . We also have

$$\begin{aligned} \left(\frac{\partial h}{\partial x} \dot{x} + \gamma y \right) &= \frac{\partial h}{\partial x} [f(x) + G(x)\psi(x)] - \frac{\alpha(x)}{\mu} M(x)(y + \gamma\bar{\sigma}) \\ &\quad - M(x) \frac{\delta(0)}{\alpha(0)} [\alpha(x) - \alpha(0)] + M(x) [\bar{\delta}(x) - \psi(x)] + \gamma y. \end{aligned}$$

Since $x \in \{V(x) \leq \rho(\mu)\}$, $\alpha(x)$ and $\|M(x)\|$ can be bounded by constants. Moreover, since $M(0) + M^T(0)$ is positive definite, there is a positive constant $c_2 \leq c_1$ such that

$M(x) + M^T(x)$ is positive definite for all $x \in \Omega_1 = \{V(x) \leq c_2\} \subset \Omega$. Let

$$\lambda_q = \frac{1}{2} \min_{x \in \Omega_1} \lambda_{\min} \{M(x) + M^T(x)\}. \quad (2.23)$$

For sufficiently small μ , $\{V(x) \leq \rho(\mu)\} \subset \Omega_1$, hence

$$M(x) + M^T(x) \geq 2\lambda_q I, \quad \forall x \in \{V(x) \leq \rho(\mu)\}. \quad (2.24)$$

Using (2.24) and Assumption 4 we obtain

$$\begin{aligned} (y + \gamma\tilde{\sigma})^T \left(\frac{\partial h}{\partial x} \dot{x} + \gamma y \right) &\leq -\frac{\alpha(x)}{\mu} \lambda_q \|(y + \gamma\tilde{\sigma})\|^2 + k_{11} \|y\| \sqrt{W(x)} \\ &\quad + k_{12} \|\tilde{\sigma}\| \sqrt{W(x)} + k_{12} \|y\|^2 + k_{10} \|\tilde{\sigma}\| \|y\|, \end{aligned}$$

where $k_{10}, k_{11}, k_{12}, k_{12} \geq 0$. Therefore,

$$\begin{aligned} \dot{V}_2 &\leq -\frac{W(x)}{2} - \alpha(x) \frac{\lambda}{\mu} \|y\|^2 + (k_7 + ck_{12}) \|y\|^2 + (k_8 + ck_{11}) \|y\| \sqrt{W(x)} - \frac{W(x)}{2} \\ &\quad + b\tilde{\sigma}^T y - c \frac{\alpha(x)}{\mu} \lambda_q \|(y + \gamma\tilde{\sigma})\|^2 + ck_{12} \|\tilde{\sigma}\| \sqrt{W(x)} - \alpha(x) y^T L(x) \gamma \frac{\tilde{\sigma}}{\mu} \\ &\quad + ck_{10} \|\tilde{\sigma}\| \|y\|. \end{aligned}$$

Taking $b = 2c\lambda_q \gamma \frac{\alpha(0)}{\mu}$, we can express the upper bound on \dot{V}_2 as

$$\dot{V}_2 \leq -W_1(x) - W_2(x) - W_3(x),$$

where

$$\begin{aligned}
W_1(x) &= \frac{W(x)}{2} + \|y\|^2 \left(\frac{\alpha_{min}}{\mu} \lambda - k_7 - ck_{12} \right) - (k_8 + ck_{11}) \|y\| \sqrt{W(x)} \\
W_2(x) &= \frac{W(x)}{2} + c\alpha_{min} \gamma^2 \frac{\lambda_q}{2\mu} \|\tilde{\sigma}\|^2 - ck_{12} \|\tilde{\sigma}\| \sqrt{W(x)}, \quad \alpha_{min} = \min_{x \in \Omega} \alpha(x) \\
W_3(x) &= \frac{\alpha(x)}{\mu} \left\{ c\lambda_q \|y\|^2 + \frac{c}{2} \gamma^2 \lambda_q \|\tilde{\sigma}\|^2 - \left[\gamma k + \frac{(2c\lambda_q \gamma \rho_2(\mu) + ck_{10}\mu)}{\alpha_{min}} \right] \|\tilde{\sigma}\| \|y\| \right\}
\end{aligned}$$

and ρ_2 is a class \mathcal{K} function such that

$$\|\alpha(x) - \alpha(0)\| \leq \rho_2(\mu), \quad \forall x \in \{V(x) \leq \rho(\mu)\}.$$

We can see that both $W_1(x)$ and $W_2(x)$ will be positive definite for sufficiently small μ . For $W_3(x)$ to be positive definite, we need

$$\frac{c^2}{2} \gamma^2 \lambda_q^2 > \frac{1}{4} \left[\gamma k + \frac{(2c\lambda_q \gamma \rho_2(\mu) + ck_{10}\mu)}{\alpha_{min}} \right]^2.$$

Taking $c = k/\lambda_q$ ensures that \dot{V}_2 will be negative definite for sufficiently small μ ; consequently the equilibrium point $\left(x = 0, \bar{\sigma} = \frac{\mu}{\alpha(0)\gamma} \delta(0) \right)$ will be asymptotically stable for sufficiently small μ .

b) Inequality (2.18) is valid $\forall (x, \sigma) \in R^n \times \{\|\sigma\| \leq \mu/\gamma\}$. Using (2.5) and (2.17) we obtain

$$\dot{V} \leq -W(x) + 3k\alpha(x)\mu$$

$$\leq -[1 - 3\mu k_g k]W(x) + 3k c_g \mu.$$

Hence, as in part a), for sufficiently small μ , all trajectories starting in $(x, \sigma) \in \{V(x) \leq c_1\} \times \{\|\sigma\| \leq \mu/\gamma\}$ enter Σ_μ . Since $V(x)$ is radially unbounded, c_1 can be chosen to include any $x(0) \in R^n$ in the set $\{V(x) \leq c_1\}$. Analysis inside the set Σ_μ remains the same as in part a). Thus, for sufficiently small $\mu, \forall x(0) \in R^n$ and $\|\sigma(0)\| \leq \mu/\gamma, x(t) \rightarrow 0$ as $t \rightarrow \infty$.

Remark: In Theorem 1 we assumed $\|\sigma(0)\| \leq \mu/\gamma$. However, we can relax this requirement. Given $\|\sigma(0)\| \leq k_\sigma/\gamma, k_\sigma \geq \mu$, then, from (2.9),

$$\sigma^T \dot{\sigma} \leq -\frac{\gamma}{2}\|\sigma\|^2, \quad \forall \|\sigma\| \geq \frac{2\mu}{\gamma}.$$

Hence, from ([11], Theorem 4.18), $\sigma(t)$ reaches the set $\{\|\sigma\| \leq 2\mu/\gamma\}$ in finite time.

For $\|\sigma(0)\| \leq k_\sigma/\gamma$ we can repeat the derivation preceding (2.18) to show that

$$\dot{V} \leq -W(x) + \alpha_2 k_\sigma, \quad \forall x \in \Omega.$$

Thus, from ([11], Theorem 4.18), there exists a positively invariant set $\mathcal{S} = \{V(x) \leq \rho_3(k_\sigma)\}$, where ρ_3 is a class \mathcal{K} function, such that trajectories starting outside \mathcal{S} reach it in finite time. If k_σ is small enough such that $\mathcal{S} \subset \Omega$, then $x(0) \in \Omega \implies x(t) \in \Omega, \forall t \geq 0$. Once $\|\sigma\|$ reaches the set $\{\|\sigma\| \leq 2\mu/\gamma\}$ the proof of Theorem 1 can be repeated for the set $\Omega \times \{\|\sigma\| \leq 2\mu/\gamma\}$.

2.4 Performance

In this section we show that the conditional integrator does not degrade the transient response of the system, in the sense that, as $\mu \rightarrow 0$, the trajectory of the closed loop system under saturated high-gain feedback with conditional integrator (2.8) approach those of the closed-loop system under saturated high-gain feedback without integrator (2.7). The closed-loop system under (2.8) is represented by (2.4), (2.8), (2.9) while the closed-loop system under (2.7) is given by

$$\dot{x}^* = f(x^*) + G(x^*)\delta(x^*) - \alpha(x^*)G(x^*)\varphi\left(\frac{y^*}{\mu}\right), \quad (2.25)$$

where $y^* = h(x^*)$. In both cases, the trajectories eventually enter a boundary layer, which is $\{\|y + \gamma\sigma\| \leq \mu\}$ for (2.4), (2.8), (2.9) and $\{\|y^*\| \leq \mu\}$ for (2.25). Showing closeness of trajectories is relatively easy when trajectories of both systems are either outside or inside their respective boundary layers. The tricky part is to keep track of the closeness of trajectories as trajectories enter and leave the boundary layers since the entry and exit times will be different for the two systems. Note that, while trajectories eventually settle inside the boundary layers, there could be a period of time when trajectories go in and out for a finite number of times. For convenience, we restrict our analysis to a case where once the trajectories enter the boundary layers, they cannot leave. This will require us to limit the compact set of analysis and to change the choice of the function $\alpha(x)$ in the feedback control law (2.7) or (2.8).

Recall from the proof of Theorem 1 that $\Omega_1 = \{V(x) \leq c_2\} \subset \Omega$ is a compact set such that $M^T(x) + M(x)$ is positive definite in Ω_1 . Let λ_q be defined by (2.23) and

$$k_q = \max_{x \in \Omega_1} \|M(x)\|.$$

Let $\beta_1(x)$ be a known continuous function such that

$$\left\| \frac{\partial h}{\partial x} [f(x) + G(x)\psi(x)] \right\| \leq \beta_1(x), \quad \forall x \in \Omega_1.$$

The choice of $\alpha(x)$ is changed to

$$\alpha(x) \geq \max \left\{ \frac{k}{\lambda} \beta(x), \frac{k_q}{\lambda_q} \beta(x) + \frac{1}{\lambda_q} \beta_1(x) \right\} + \alpha_0. \quad (2.26)$$

The choice (2.26) is more conservative than (2.5); hence, the conclusions of Theorem 1 hold for all $x(0) \in \Omega_1$. For all (x, σ) in the positively invariant set $\Omega_1 \times \{\|\sigma\| \leq \mu/\gamma\}$, the derivative of $V_1 = \frac{1}{2}\|y + \gamma\sigma\|^2$ satisfies

$$\begin{aligned} \dot{V}_1 &= (y + \gamma\sigma)^T (\dot{y} + \gamma\dot{\sigma}) \\ &\leq -\alpha(x)(y + \gamma\sigma)^T M(x) \varphi \left(\frac{y + \gamma\sigma}{\mu} \right) + [\beta_1(x) + k_q \beta(x) + 2\gamma\mu] \|y + \gamma\sigma\|. \end{aligned}$$

Outside the boundary layer $\{\|y + \gamma\sigma\| \leq \mu\}$, we have

$$\dot{V}_1 \leq -\lambda_q \left[\alpha_0 - \frac{2\gamma\mu}{\lambda_q} \right] \|y + \gamma\sigma\|.$$

Hence, for sufficiently small μ , all trajectories starting inside $\Omega_1 \times \{\|\sigma\| \leq \mu/\gamma\}$ will reach the boundary layer $\{\|y + \gamma\sigma\| \leq \mu\}$ in finite time and stay there for all future time. We can arrive at a similar conclusion for the system (2.25) using $V_2 = \frac{1}{2}\|y^*\|^2$.

To compare the equations of the two systems inside the boundary layers, it is convenient to recognize that high-gain feedback creates slow and fast dynamics, which can be represented in the singularly perturbed form. The following two assumptions are used in analyzing the closeness of trajectories inside the boundary layers.

Assumption 5: There exists a diffeomorphism $T(x)$ such that

$$\frac{\partial T(x)}{\partial x} G(x) = \begin{bmatrix} 0 \\ I \end{bmatrix},$$

$\forall x \in \Omega_1$.

The change of variables $z = \begin{bmatrix} z_1 \\ z_2 \end{bmatrix} = T(x)$ transforms the system (2.1) into

$$\dot{z}_1 = f_1^\dagger(z_1, z_2)$$

$$\dot{z}_2 = f_2^\dagger(z_1, z_2) + u$$

and $y = h(x)_{x=T^{-1}(z)}$ can be written as $y = h^\dagger(z_1, z_2)$

Assumption 6: $0 = h^\dagger(z_1, z_2)$ has a unique solution $z_2 = v(z_1)$ for all $x \in \Omega_1$ and the system

$$\dot{z}_1 = f_1^\dagger(z_1, v(z_1))$$

has an exponentially stable equilibrium point at $z_1 = 0$.

Theorem 2: Suppose Assumptions 1-6 are satisfied and $\alpha(x)$ satisfies (2.26). Let $x(t)$ and $\sigma(t)$ be the state of (2.4), (2.8), (2.9) with $x(0) \in \Omega_1$, $\|\sigma(0)\| \leq \mu/\gamma$, and $x^*(t)$ be the state of (2.25) with $x^*(0) \in \Omega_1$. Suppose that $\|x(0) - x^*(0)\| = \mathcal{O}(\mu)$. Then, $\|x(t) - x^*(t)\| = \mathcal{O}(\mu)$, $\forall t \geq 0$.

Proof : Let t_1 be the first time one of the two systems reaches its boundary layer. For all $t \leq t_1$, trajectories of both the systems are outside their respective boundary layers and the systems are represented by

$$\left. \begin{aligned} \dot{\sigma} &= -\gamma\sigma + \mu\varphi\left(\frac{y+\gamma\sigma}{\mu}\right) \\ \dot{x} &= f(x) + G(x)\delta(x) - \alpha(x)G(x)\left(\frac{y+\gamma\sigma}{\|y+\gamma\sigma\|}\right) \end{aligned} \right\} \quad (2.27)$$

$$\dot{x}^* = f(x^*) + G(x^*)\delta(x^*) - \alpha(x^*)G(x^*)\left(\frac{y^*}{\|y^*\|}\right). \quad (2.28)$$

As $\|\sigma\| = \mathcal{O}(\mu)$, the difference in the state equations for \dot{x} and \dot{x}^* is $\mathcal{O}(\mu)$ for all $t \leq t_1$. From ([11], Theorem 3.4), $\|x(t) - x^*(t)\| = \mathcal{O}(\mu)$, $\forall t \leq t_1$. From, $\|\sigma\| = \mathcal{O}(\mu)$, and $\|x(t_1) - x^*(t_1)\| = \mathcal{O}(\mu)$ it can be seen that if trajectories of one system reach its boundary layer, the trajectories of the other system will be in some $\mathcal{O}(\mu)$ neighborhood of its boundary layer. As derivatives of both $\frac{1}{2}\|(y + \gamma\sigma)\|^2$ and $\frac{1}{2}\|y^*\|^2$ are strictly negative outside their boundary layers, uniformly in μ , it must be true that trajectories of the other system also reach its boundary layer in time $t_2 = t_1 + \mathcal{O}(\mu)$. Hence, $\|x(t) - x^*(t)\| = \mathcal{O}(\mu)$, $\forall t \in [t_1, t_2]$. For all $t > t_2$, trajectories of both systems (2.27) and (2.28) are inside their respective boundary layers and can be represented by

$$\left. \begin{aligned} \dot{\sigma} &= y \\ \dot{x} &= f(x) + G(x)\delta(x) - \alpha(x)G(x) \left(\frac{y + \gamma\sigma}{\mu} \right) \end{aligned} \right\} \quad (2.29)$$

$$\dot{x}^* = f(x^*) + G(x^*)\delta(x^*) - \alpha(x^*)G(x^*) \left(\frac{y^*}{\mu} \right). \quad (2.30)$$

With the change of variables $z = \begin{bmatrix} z_1 \\ z_2 \end{bmatrix} = T(x)$ and $z^* = \begin{bmatrix} z_1^* \\ z_2^* \end{bmatrix} = T(x^*)$, (2.29) and (2.30) can be written in the singularly perturbed forms

$$\left. \begin{aligned} \dot{\sigma} &= h^\dagger(z_1, z_2) \\ \dot{z}_1 &= f_1^\dagger(z_1, z_2) \\ \mu \dot{z}_2 &= \mu[f_2^\dagger(z_1, z_2) + \delta^\dagger(z_1, z_2)] - \alpha^\dagger(z_1, z_2)[h^\dagger(z_1, z_2) + \gamma\sigma] \end{aligned} \right\} \quad (2.31)$$

$$\left. \begin{aligned} \dot{z}_1^* &= f_1^\dagger(z_1^*, z_2^*) \\ \mu \dot{z}_2^* &= \mu[f_2^\dagger(z_1^*, z_2^*) + \delta^\dagger(z_1^*, z_2^*)] - \alpha^\dagger(z_1^*, z_2^*)h^\dagger(z_1^*, z_2^*) \end{aligned} \right\}, \quad (2.32)$$

where $\delta^\dagger(z_1, z_2) = \delta(x)|_{x=T^{-1}(z)}$, $\alpha^\dagger(z_1, z_2) = \alpha(x)|_{x=T^{-1}(z)}$ and $h^\dagger(z_1, z_2) = h(x)|_{x=T^{-1}(z)}$. Let $z_2 = v_1(z_1, \sigma)$ be the unique solution to $h^\dagger(z_1, z_2) + \gamma\sigma = 0$.

The slow and fast models of (2.31) and (2.32) are given by

$$\left. \begin{aligned} \dot{\sigma} &= -\gamma\sigma \\ \dot{z}_1 &= f_1^\dagger(z_1, v_1(z_1, \sigma)) \end{aligned} \right\} \quad (2.33)$$

$$\frac{dz_2}{d\tau} = -\alpha^\dagger(z_1, z_2)[h^\dagger(z_1, z_2) + \gamma\sigma] \quad (2.34)$$

$$\dot{z}_1^* = f_1^\dagger(z_1^*, v_1(z_1^*)) \quad (2.35)$$

$$\frac{dz_2^*}{d\tau} = -\alpha^\dagger(z_1^*, z_2^*)h^\dagger(z_1^*, z_2^*), \quad (2.36)$$

where $\tau = t/\mu$. The differences between the right hand sides of the slow models (2.33), (2.35) and the fast models (2.34), (2.36) are $\mathcal{O}(\mu)$. Furthermore, from Assumptions 3 and 6 it can be verified that systems (2.33), (2.34), (2.35), and (2.36) are exponentially stable. Hence, from ([11], Theorem 9.1) and Tikhonov theorem ([11], Theorem 11.2), $\|x(t) - x^*(t)\| = \mathcal{O}(\mu)$, $\forall t \geq t_2$. Thus, $\|x(t) - x^*(t)\| = \mathcal{O}(\mu)$, $\forall t \geq 0$.

Example: Consider the second-order system

$$\left. \begin{aligned} \dot{x}_1 &= -x_1 - x_2 \\ \dot{x}_2 &= x_1 + u \end{aligned} \right\}. \quad (2.37)$$

Assumption 1 is satisfied with $\psi(x) = -x_2$, $V(x) = (x_1^2 + x_2^2)/2$, $W(x) = -x_1^2 - x_2^2$ and Assumption 2 is satisfied with $h(x) = x_2$, $L(x) = 1$. It can be easily verified that $M^T(x) + M(x)$ is positive definite $\forall x \in R^2$ and Assumptions 3-6 are also satisfied. A constant matched uncertainty $\delta(x) = 1$ is added to the control u to shift the equilibrium point from the origin. To recover asymptotic stability of the origin, system (2.37) is augmented with the conditional integrator (2.9) and from (2.8) and (2.26), the control u is given by

$$u = -(2|x_2| + |x_1| + 2.2) \text{sat}\left(\frac{x_2 + \sigma}{\mu}\right).$$

The closed-loop system can be written as

$$\left. \begin{aligned} \dot{\sigma} &= -\gamma\sigma + \mu \text{sat}\left(\frac{x_2 + \sigma}{\mu}\right) \\ \dot{x}_1 &= -x_1 - x_2 \\ \dot{x}_2 &= x_1 + u + 1 \\ u &= -(2|x_2| + |x_1| + 2.2) \text{sat}\left(\frac{x_2 + \sigma}{\mu}\right) \end{aligned} \right\}. \quad (2.38)$$

We will now demonstrate through simulation that as $\mu \rightarrow 0$, trajectories of the system (2.38) approach the trajectories of the closed-loop system

$$\left. \begin{aligned} \dot{x}_1^* &= -x_1^* - x_2^* \\ \dot{x}_2^* &= x_1^* + u + 1 \\ u &= -(2|x_2^*| + |x_1^*| + 2.2) \text{sat}\left(\frac{x_2^*}{\mu}\right) \end{aligned} \right\}. \quad (2.39)$$

Simulation was run for the initial conditions $x_1(0) = x_1^*(0) = 0$, $x_2(0) = x_2^*(0) = -20$

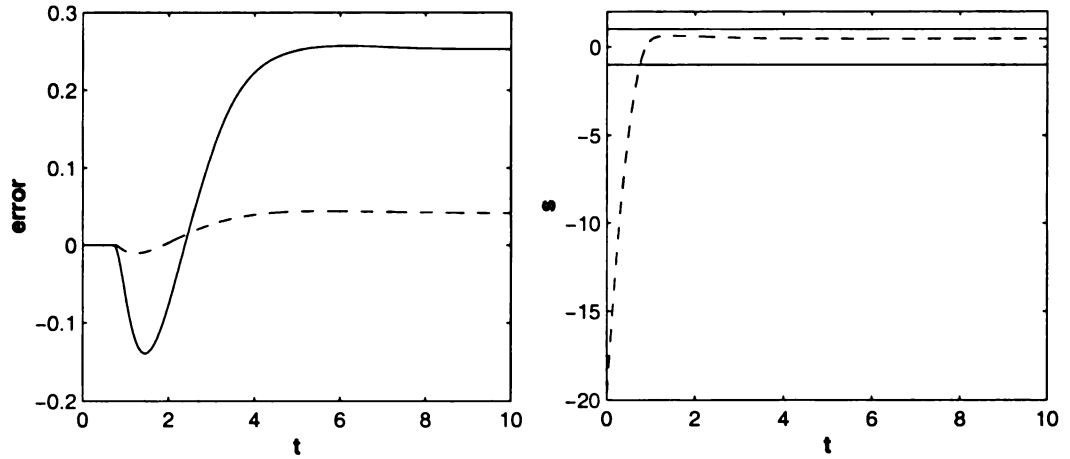


Figure 2.2. Plot of error $\|x_1(t) - x_1^*(t)\|$ for systems (2.38) and (2.39) with $\mu = 1$ (solid), $\mu = .1$ (dashed) and plot of $s = \|y + \sigma\|$ (dashed) for $\mu = 1$, with initial conditions $x_1(0) = x_1^*(0) = 0, x_2(0) = x_2^*(0) = -20$ and $\sigma(0) = 0$

and $\sigma(0) = 0$, for different values of μ . It can be seen from Figure 2.2 that the trajectories of (2.38) enter its boundary layer and stay there for all future time, and that they approach those of (2.39) as $\mu \rightarrow 0$. However, if $\alpha(x)$ is given by (2.5), as was taken in Theorem 1, in place of (2.26) then the control u would be

$$u = -(|x_2| + 2.2) \text{sat}\left(\frac{x_2 + \sigma}{\mu}\right).$$

The closed-loop systems (2.38) and (2.39) would be

$$\left. \begin{aligned} \dot{\sigma} &= -\gamma\sigma + \mu \text{sat}\left(\frac{x_2 + \sigma}{\mu}\right) \\ \dot{x}_1 &= -x_1 - x_2 \\ \dot{x}_2 &= x_1 + u + 1 \\ u &= -(|x_2| + 2.2) \text{sat}\left(\frac{x_2 + \sigma}{\mu}\right) \end{aligned} \right\} \quad (2.40)$$

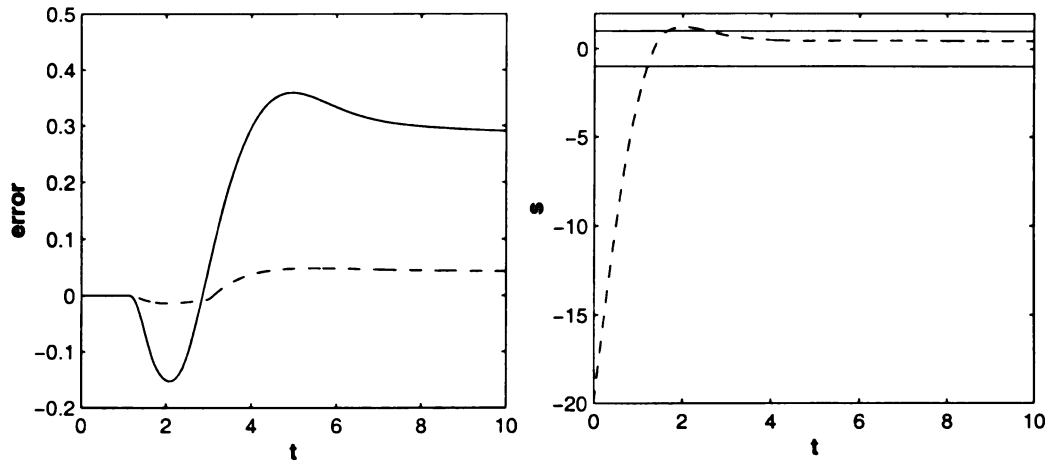


Figure 2.3. Plot of error $\|x_1(t) - x_1^*(t)\|$ for systems (2.40) and (2.41) with $\mu = 1$ (solid), $\mu = .1$ (dashed) and plot of $s = \|y + \sigma\|$ (dashed) for $\mu = 1$, with initial conditions $x_1(0) = x_1^*(0) = 0, x_2(0) = x_2^*(0) = -15$ and $\sigma(0) = 0$

and

$$\left. \begin{aligned} \dot{x}_1^* &= -x_1^* - x_2^* \\ \dot{x}_2^* &= x_1^* + u + 1 \\ u &= -(|x_2^*| + 2.2) \text{sat}\left(\frac{x_2^*}{\mu}\right) \end{aligned} \right\}. \quad (2.41)$$

For similar initial conditions $x_1(0) = x_1^*(0) = 0, x_2(0) = x_2^*(0) = -20$ and $\sigma(0) = 0$, it can be seen from Figure 2.3 that the trajectories of (2.40) enter and leave its boundary layer once before settling there; yet the trajectories of (2.40) still approach those of (2.41) as $\mu \rightarrow 0$, a property that is not guaranteed by Theorem 2.

CHAPTER 3

Output Feedback of Minimum-Phase Systems

In this section we apply the conditional integrator design of Section 2 to output feedback regulation of a class of minimum-phase, input-output linearizable systems. Aside from some technical differences, this is the same problem treated in [14], but the controller design presented here is different from the “continuous” sliding mode controller of [14].

3.1 Problem Statement

Consider the MIMO nonlinear system

$$\dot{x} = f(x, w) + G(x, w)u \quad (3.1)$$

$$y = l(x, w) \quad (3.2)$$

where $u \in R^m$ is the control input, $x \in R^n$ is the state vector, $y \in R^m$ is the measured output and the disturbance input w belongs to a compact set $\mathcal{W} \subset R^l$. The functions $G(x, w), f(x, w), l(x, w)$ are sufficiently smooth functions in x on a domain $\mathcal{X} \subset R^n$ and continuous in w for $w \in \mathcal{W}$. We want to regulate $y(t) \rightarrow 0$ as $t \rightarrow \infty$. We make the following Assumptions about (3.1), (3.2).

Assumption 7: For each $w \in \mathcal{W}$ there is a unique pair (x_{ss}, u_{ss}) that depends continuously on w and satisfies

$$0 = f(x_{ss}, w) + G(x_{ss}, w)u_{ss} \quad (3.3)$$

$$0 = l(x_{ss}, w). \quad (3.4)$$

Subtracting (3.3) from (3.1), we have

$$\dot{x} = \tilde{f}(x, w) + G(x, w)[u - u_{ss}], \quad (3.5)$$

where $\tilde{f}(x, w) = f(x, w) - f(x_{ss}, w) + [G(x, w) - G(x_{ss}, w)]u_{ss}$. Hence, the regulation problem reduces to the stabilization of the equilibrium point $x = x_{ss}$. The system (3.5) is in the form (2.4) with u_{ss} as the matched uncertainty δ .

Assumption 8: For all $w \in \mathcal{W}$ there exists a mapping

$$\begin{bmatrix} \eta \\ \zeta \end{bmatrix} = T_w(x)$$

which is a diffeomorphism over \mathcal{X} onto its image $\mathcal{X}_\eta \times \mathcal{X}_\zeta$, that transforms (3.5), (3.2) into the normal form

$$\left. \begin{aligned} \dot{\eta} &= \phi(\eta, \zeta, w) \\ \dot{\zeta} &= A\zeta + B\{b(\eta, \zeta, w) + D(\eta, \zeta, w)[u - u_{ss}]\} \\ y &= C\zeta \end{aligned} \right\} \quad (3.6)$$

and maps the equilibrium point x_{ss} into $(\eta_{ss}, 0)$ with η and ζ belonging to the sets $\mathcal{X}_\eta \subset R^{n-r}$ and $\mathcal{X}_\zeta \subset R^r$ respectively. The $m \times m$ matrix $D(\eta, \zeta, w)$ is non-singular for all $(\eta, \zeta, w) \in \mathcal{X}_\eta \times \mathcal{X}_\zeta \times \mathcal{W}$. The $r \times r$ matrix A and the $r \times m$ matrix B are given by (2.13) and (2.15), respectively. The $m \times r$ matrix C is given by

$$C = \text{block diag}[C_1, \dots, C_m], \quad (3.7)$$

$$C_i = \begin{bmatrix} 1 & 0 & \dots & \dots & 0 \end{bmatrix}_{1 \times r_i}, \quad (3.8)$$

where $1 \leq i \leq m$ and $r = r_1 + \dots + r_m$. The triple (A, B, C) represents m chains of integrators.

Conditions for the existence of such a change of variables that transform (3.5), (3.2) into the normal form (3.6) are discussed in ([8], Chapters 5 and 9)

Assumption 9: For all $(\eta, \zeta, w) \in \mathcal{X}_\eta \times \mathcal{X}_\zeta \times \mathcal{W}$,

$$D(\eta, \zeta, w) + D^T(\eta, \zeta, w) > 0 \quad (3.9)$$

$$B^T P B D(\eta_{ss}, 0, w) + D^T(\eta_{ss}, 0, w) B^T P B > 0 \quad (3.10)$$

where $P = P^T$ is the solution of the Lyapunov equation $P(A - BK) + (A - BK)^T P = -Q$ in which Q is a positive definite matrix and $A - BK$ is Hurwitz.

In [14], Assumption 5, the decoupling matrix $D(\eta, \zeta, w)$, is required to be of the form

$$D(\eta, \zeta, w) = \Gamma(\eta, \zeta, w) \hat{A}(\zeta, w), \quad (3.11)$$

where \hat{A} is a known nonsingular matrix and $\Gamma = \text{diag}[\gamma_1, \dots, \gamma_m]$ with $\gamma_i(\cdot) \geq \gamma_0 > 0$, $1 \geq i \geq m$, for all $(\eta, \zeta, w) \in \mathcal{X}_\eta \times \mathcal{X}_\zeta \times \mathcal{W}$ and some positive constant γ_0 . In the case of (3.11), without loss of generality a new control input can be defined as $v = \hat{A}(\zeta, w)u$ and with respect to the input v , the decoupling matrix $D(\eta, \zeta, w) = \Gamma(\eta, \zeta, w)$ will satisfy (3.9).

Assumption 10: There exists a Lyapunov function $V_r(\bar{\eta}, w)$ where $\bar{\eta} = \eta - \eta_{ss}$ and

a compact set $\mathcal{X}_w \subset \mathcal{X}_\eta \times \mathcal{X}_\zeta \times \mathcal{W}$ such that $\forall (\eta, \zeta, w) \in \mathcal{X}_w$

$$\frac{\partial V_r(\bar{\eta}, w)}{\partial \bar{\eta}} \phi(\eta, \zeta, w) \leq -k_{15} \|\bar{\eta}\|^2 + k_{16} \|\bar{\eta}\| \|\zeta\|$$

for some constants $k_{15} > 0, k_{16} \geq 0$.

With $\phi(\eta, \zeta, w)$ being locally Lipschitz in its arguments, if $\eta = \eta_{ss}$ is an exponentially stable equilibrium point of $\dot{\eta} = \phi(\eta, 0, w)$, then, the existence of such Lyapunov function is ensured by the converse Lyapunov theorem ([11], Theorem 4.16). In [14], Assumption 4, exponential stability of $\dot{\eta} = \phi(\eta, 0, w)$ is required but the upper bound on $\frac{\partial V_r(\bar{\eta}, w)}{\partial \bar{\eta}} \phi(\eta, \zeta, w)$ does not need to be quadratic in $\|\zeta\|$ and $\|\bar{\eta}\|$ over the compact set \mathcal{X}_w .

3.2 Partial State Feedback Design

It can be seen that $\forall (\eta, \zeta, w) \in \mathcal{X}_w$, Assumption 1 is satisfied with $\psi(\bar{\eta}, \zeta, w) = D^{-1}(\bar{\eta} + \eta_{ss}, \zeta, w)[-b(\bar{\eta} + \eta_{ss}, \zeta, w) - K\zeta]$, and $V(\bar{\eta}, \zeta, w) = V_r(\bar{\eta}, w) + k_{17}\zeta^T P \zeta$, where k_{17} is chosen such that $k_{17} > k_{16}^2/4k_{15}$, and that the function $W(\bar{\eta}, \zeta, w)$ is quadratic in $\|\zeta\|$ and $\|\bar{\eta}\|$. From (3.9) it can be seen that Assumption 2 is satisfied with $h^T(\zeta) = 2k_{17}\zeta^T P B$ and $L(\bar{\eta}, \zeta, w) = D(\bar{\eta} + \eta_{ss}, \zeta, w)$. Inequality (3.10) satisfies Assumption 3 and as $W(\bar{\eta}, \zeta, w)$ is quadratic in $\|\zeta\|$ and $\|\bar{\eta}\|$ Assumption 4 is also satisfied.

Let $\beta(\zeta)$ be a known function such that $\forall (\eta, \zeta, w) \in \mathcal{X}_w$,

$$\|u_{ss} + \psi(\bar{\eta}, \zeta, w)\| \leq \beta(\zeta). \quad (3.12)$$

Then, from (2.8), a partial state feedback control is taken as

$$u = -\alpha(\zeta)\varphi\left(\frac{2k_{17}B^TP\zeta + \gamma\sigma}{\mu}\right), \quad \mu > 0, \quad (3.13)$$

where $\alpha(\zeta)$ and σ are given by (2.5) and (2.9), respectively. From Theorem 1 it can be seen that for the closed-loop system (2.9), (3.6), (3.13), for sufficiently small $\mu, \zeta \rightarrow 0$ as $t \rightarrow \infty$. Thus, $\lim_{t \rightarrow \infty} y(t) = 0$.

3.3 Output Feedback Design

The controller (3.13) cannot be implemented as a state feedback controller because the partial states ζ depends on the unknown vector w through the change of variables $T_w(x)$. However, it can be implemented as an output feedback controller that uses the high-gain observer

$$\dot{\hat{\zeta}} = A\hat{\zeta} + H(y - C\hat{\zeta}) \quad (3.14)$$

to estimate ζ , where A is given by (2.13) and the observer gain H is chosen as

$$H = \text{block diag}[H_1, \dots, H_m], \quad H_i = \begin{bmatrix} \frac{\alpha_1^i}{\epsilon} \\ \frac{\alpha_2^i}{\epsilon^2} \\ \vdots \\ \frac{\alpha_{r_i-1}^i}{\epsilon^{r_i-1}} \\ \frac{\alpha_{r_i}^i}{\epsilon^{r_i}} \end{bmatrix}_{r_i \times 1}$$

in which ϵ is a positive constant and the positive constants α_j^i are chosen such that the roots of

$$s^{r_i} + \alpha_1^i s^{r_i-1} + \dots + \alpha_{r_i}^i = 0$$

are in the open left-half plane, for all $i = 1, \dots, m$. The output feedback control is given by

$$\left. \begin{aligned} \dot{\hat{\zeta}} &= A\hat{\zeta} + H(y - C\hat{\zeta}) \\ \dot{\sigma} &= -\gamma\sigma + \mu\varphi\left(\frac{2k_{17}B^T P\hat{\zeta} + \gamma\sigma}{\mu}\right) \\ u &= -\alpha(\hat{\zeta})\varphi\left(\frac{2k_{17}B^T P\hat{\zeta} + \gamma\sigma}{\mu}\right) \end{aligned} \right\}. \quad (3.15)$$

If the closed-loop system under the state feedback control (3.13) has an exponentially stable equilibrium point at the origin then, for sufficiently small ϵ , the closed-loop system under the output feedback control (3.15) will have an exponentially stable equilibrium point [2]. If the equilibrium point is asymptotically, but not exponentially, stable we need to place an upper bound on the modeling error

$$\delta_0(\eta, \zeta, w) = b(\eta, \zeta, w) + D(\eta, \zeta, w)[u - u_{ss}].$$

In the latter case, for each w , the following properties hold. The closed-loop system under state feedback can be transformed into the form ([11], Theorem 4.7)

$$\left. \begin{aligned} \dot{\bar{\eta}} &= A_1 \bar{\eta} + g_1(\bar{\eta}, \bar{\zeta}, w) \\ \dot{\bar{\zeta}} &= A_2 \bar{\zeta} + g_2(\bar{\eta}, \bar{\zeta}, w) \end{aligned} \right\}, \quad (3.16)$$

where A_1 has all its eigenvalue with zero real parts and A_2 is Hurwitz. Also ([11], Theorem 8.1), guarantees the existence of a continuously differentiable center manifold $\bar{\zeta} = \bar{h}(\bar{\eta}, w)$ for all $\|\bar{\eta}\| \leq d_w$, for some $d_w > 0$. From ([11], Corollary 8.2) the origin of the reduced system

$$\dot{\bar{\eta}} = A_1 \bar{\eta} + g_1(\bar{\eta}, \bar{h}(\bar{\eta}, w), w) = g_0(\bar{\eta}, w) \quad (3.17)$$

is asymptotically stable and the converse Lyapunov theorem ([11], Theorem 4.16) guarantees the existence of a continuously differentiable function $V_3(\bar{\eta}, w)$ defined on

$B_{\bar{\eta}}(0, r)$, a ball of radius r around $\bar{\eta} = 0$, such that $\forall \bar{\eta} \in B_{\bar{\eta}}(0, r)$,

$$\frac{\partial V_3}{\partial \bar{\eta}} g_0(\bar{\eta}, w) \leq -\alpha_0(\|\bar{\eta}\|),$$

where α_0 is a class \mathcal{K} function, possibly dependent on w .

For the above properties to hold uniformly in $w \in \mathcal{W}$, we make the following assumptions.

Assumption 11: The closed-loop system under state feedback can be transformed into the form (3.16), where A_1 has all its eigenvalue with zero real parts and A_2 is Hurwitz, uniformly in $w \in \mathcal{W}$.

Assumption 12: There exist a continuously differentiable center manifold $\bar{\zeta} = \bar{h}(\bar{\eta}, w)$ for all $\|\bar{\eta}\| \leq d_w$, for some $d_w > 0$, such that origin of the system (3.17) is asymptotically stable, uniformly in $w \in \mathcal{W}$.

Assumption 13: There exist a continuously differentiable function $V_3(\bar{\eta}, w)$ defined on $B_{\bar{\eta}}(0, r)$, a ball of radius r around $\bar{\eta} = 0$, such that $\forall \bar{\eta} \in B_{\bar{\eta}}(0, r), \forall w \in \mathcal{W}$,

$$\frac{\partial V_3}{\partial \bar{\eta}} g_0(\bar{\eta}, w) \leq -\alpha_0(\|\bar{\eta}\|),$$

where α_0 is a class \mathcal{K} function, possibly dependent on w .

Let $\delta_1(\bar{\eta}, w)$ be the projection of the modeling error onto the center manifold, i.e.

$$\delta_0(\eta, \zeta, w) = \delta_1(\bar{\eta}, w) + \delta_2(\bar{\eta}, \bar{\zeta}, w),$$

where $\delta_2(\bar{\eta}, 0, w) = 0$. Now we make the following assumption on the functions $V_3(\bar{\eta}, w)$ and $\delta_1(\bar{\eta}, w)$.

Assumption 14: $\forall \bar{\eta} \in B_{\bar{\eta}}(0, r), \forall w \in \mathcal{W}$

$$\|\delta_1(\bar{\eta}, w)\| \leq c_0 \alpha_0^a(\|\bar{\eta}\|) \text{ and } \left\| \frac{\partial V_3}{\partial \bar{\eta}} \right\| \leq c_1 \alpha_0^b(\|\bar{\eta}\|),$$

where $a, b < 1$ are some positive constants such that $a + b = 1, c_0 \geq 0$ and $c_1 > 0$.

Under Assumption 14, from [2], the closed loop system under output feedback will have an asymptotically stable equilibrium point for sufficiently small ϵ .

Furthermore, from [2], if \mathcal{R} is the region of attraction under state feedback control, then for any compact set \mathcal{M} in the interior of \mathcal{R} and any compact set $\mathcal{Q} \subseteq R^r$ of initial estimate $\hat{\zeta}(0)$, the set $\mathcal{M} \times \mathcal{Q}$ is included in the region of attraction under output feedback control for sufficiently small ϵ , and trajectories under output

feedback approach those under state feedback as $\epsilon \rightarrow 0$.

3.4 Comparison of Controllers

In this section we compare the controller design presented in Section 3.2 to that of [14] through an example.

Example: Consider the two-input, third-order system

$$\left. \begin{aligned} \dot{x}_1 &= x_2 \\ \dot{x}_2 &= a_1 x_3^2 + u_1 \\ \dot{x}_3 &= a_2 x_1^2 + u_2 \\ y &= \begin{bmatrix} x_1 \\ x_3 \end{bmatrix} \end{aligned} \right\}, \quad (3.18)$$

where a_1 and a_2 are unknown constants with $|a_1| \leq 1$ and $|a_2| \leq 1$. It can be seen that Assumption 1 and 2 are satisfied with

$$\begin{aligned} \psi(x) &= \begin{bmatrix} -a_1 x_3^2 - x_1 - 2x_2 \\ -a_2 x_1^2 - x_3 \end{bmatrix}, \quad h(x) = \begin{bmatrix} x_1 + x_2 \\ 500x_3 \end{bmatrix}, \quad (3.19) \\ V(x) &= 1.5x_1^2 + 0.5x_2^2 + x_1x_2 + 250x_3^2, \quad W(x) = -x_1^2 - x_2^2 - 500x_3^2, \quad L(x) = 1. \end{aligned}$$

From (3.12) and (3.19) a function $\alpha(x)$ can be chosen as

$$\alpha(x) = \sqrt{(|x_1| + 2|x_2| + x_3^2)^2 + (x_1^2 + |x_3|)^2} + 2$$

and from (2.8) the control u can be taken as

$$u = \begin{bmatrix} u_1 \\ u_2 \end{bmatrix} = -\alpha(x)\varphi\left(\frac{h(x) + \sigma}{\mu}\right) \quad (3.20)$$

$$\dot{\sigma} = -\sigma + \mu\varphi\left(\frac{y + \sigma}{\mu}\right),$$

where $\sigma = \begin{bmatrix} \sigma_1 \\ \sigma_2 \end{bmatrix}$.

Now we will design a “continuous” sliding mode controller as presented in [14]. The first step in a sliding mode design is to specify a sliding surface on which the sliding motion occurs. The sliding surfaces are taken as

$$s_1 = x_1 + x_2 + \sigma_1$$

$$s_2 = x_3 + \sigma_2,$$

where σ_i is the output of

$$\dot{\sigma}_i = -\sigma_i + \mu_i \operatorname{sat}\left(\frac{s_i}{\mu_i}\right), \quad \sigma_i(0) \in [-\mu_i, \mu_i], \quad 1 \leq i \leq 2$$

and μ_i are positive constants to be chosen.

From ([14], (12)), a control u can be taken as

$$u = \begin{bmatrix} u_1 \\ u_2 \end{bmatrix} = - \begin{bmatrix} (x_3^2 + |x_2| + 20) \text{sat} \left(\frac{s_1}{\mu_1} \right) \\ (x_1^2 + 1) \text{sat} \left(\frac{s_2}{\mu_2} \right) \end{bmatrix}. \quad (3.21)$$

Simulation was run for the following initial conditions $x_1(0) = -3, x_2(0) = -15, x_3(0) = 1, \sigma_1(0) = 0$, and $\sigma_2(0) = 0$ with $\mu = \mu_1 = \mu_2 = .1$. The difference in performance of controllers (3.20) and (3.21) can be seen in Figure 3.1. The controller (3.20) regulates the states x_1 and x_3 faster as compared to the sliding mode controller (3.21). The control inputs u_1 and u_2 are shown in Figure 3.2.

From this example its clear that the controller design of Section 3.2 is a good alternative to the sliding mode controller design presented in [14] and can give better performance in some cases.

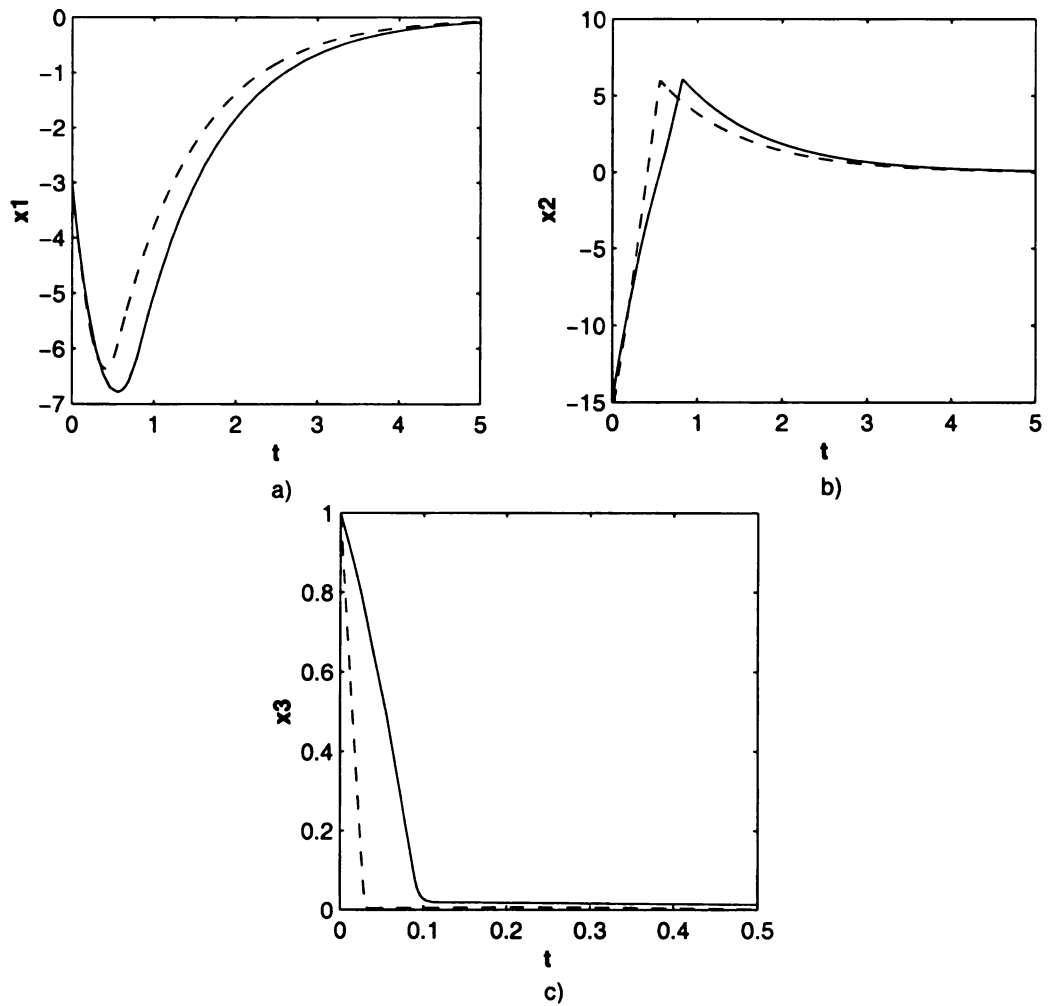


Figure 3.1. Plots of $x_1(t)$, $x_2(t)$ and $x_3(t)$ for the controller design (3.20) (dashed) and the controller design using sliding mode control (solid)

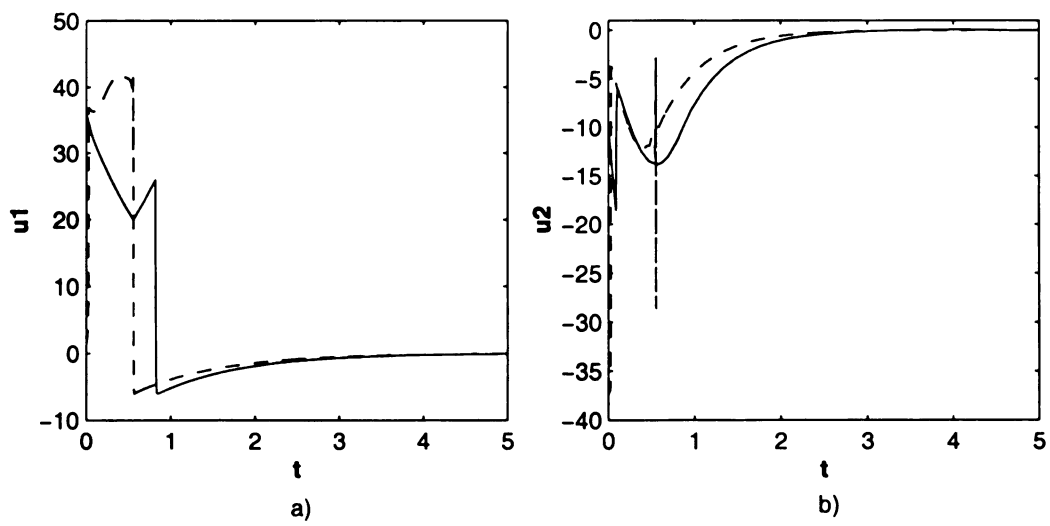


Figure 3.2. Plots of $u_1(t)$ and $u_2(t)$ for the controller design (3.20) (dashed) and the controller design using sliding mode control (solid)

CHAPTER 4

Application to the Pendubot

We illustrate the improvement in the transient response using conditional integrators by application to the Pendubot.

4.1 The Pendubot

The Pendubot is an electro-mechanical system consisting of two rigid aluminum links interconnected by a revolute joints. The first joint is actuated by a DC-motor while the second joint is unactuated, thus making the Pendubot an under actuated mechanism.

The Pendubot is in some ways, similar to the inverted pendulum on a cart, where the linear motion of the cart is used to balance the pendulum. The Pendulum uses instead the rotational motion of the first link to balance the second link. In this regard, the Pendubot is also similar to the more recent rotational inverted pendulum, invented by Professor Furuta of the Tokyo Institute of Technology [6]. In the

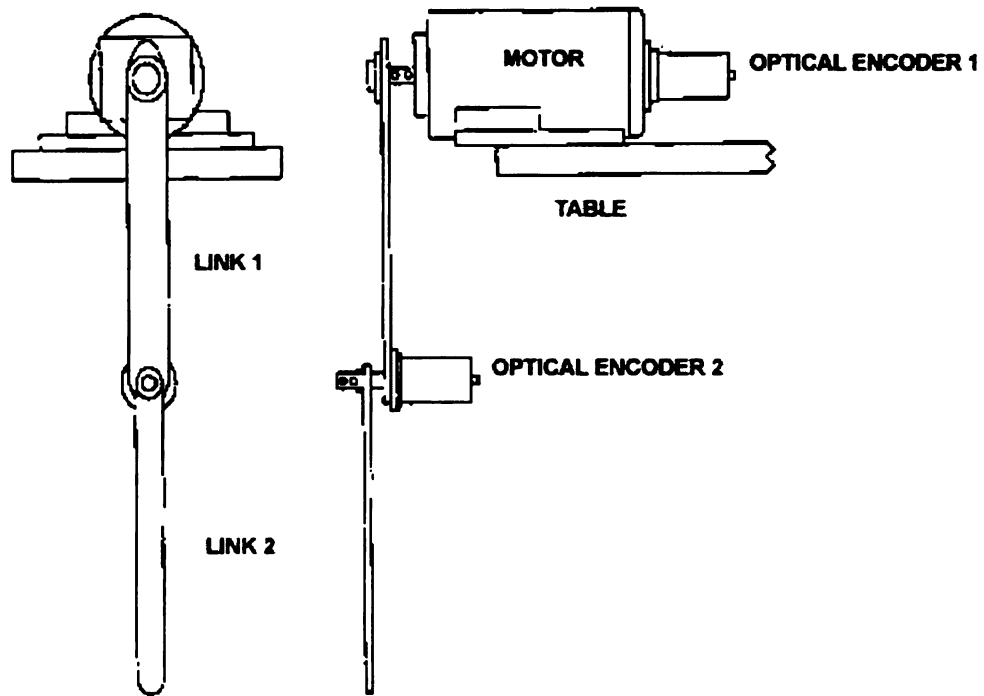


Figure 4.1. Front and side view drawing of the Pendubot.

rotational inverted pendulum, the axis of rotation of the pendulum is perpendicular to the axis of rotation of the first link. The Pendubot has both joint axes parallel, which results in some additional rotational coupling between the degrees of freedom. This additional coupling, which is not found in either the linear inverted pendulum or the rotational inverted pendulum makes the Pendubot more interesting and more challenging from both a kinematics and a dynamic stand points. For example, in both the linear inverted pendulum and the rotational inverted pendulum, the Taylor series linearization around any operating point results in a controllable linear system. Moreover, the linearized model (A, B, C) is the same at all points. In the Pendubot, the linearization is operating-point-dependent; in other words, the linearization

(A, B, C) changes at each configuration and there are even special configurations where the linearization is uncontrollable.

The Pendubot possesses many attractive features for control research and education. It can be used to investigate system identification, linear control, nonlinear control, optimal control, learning control, robust and adaptive control, fuzzy logic control, intelligent control, hybrid and switching control, gain scheduling and other control paradigms. One can program the Pendubot for swing up control, balancing, regulation, tracking, identification, gain scheduling, disturbance rejection and friction compensation to name just a few of the applications. Some of these applications are described in [18], [15] and [16]. The maker of the Pendubot is Mechatronics Systems, Inc. Figure 4.1 shows the front and side view of the Pendubot.

4.2 Mathematical Model

The equation of motion of the Pendubot can be found using Lagrangian dynamics [17]. In matrix form the equation is

$$D(q)\ddot{q} + C(q, \dot{q})\dot{q} + g(q) = u \quad (4.1)$$

where

$$\begin{aligned}
 D(q) &= \begin{bmatrix} \theta_1 + \theta_2 + 2\theta_3 \cos(q_2) & \theta_2 + \theta_3 \cos(q_2) \\ \theta_2 + \theta_3 \cos(q_2) & \theta_2 \end{bmatrix}, \\
 C(q, \dot{q}) &= \begin{bmatrix} -\theta_3 \sin q_2 \dot{q}_1 & -\theta_3 \sin(q_2)(\dot{q}_1 + \dot{q}_2) \\ \theta_3 \sin(q_2) \dot{q}_1 & 0 \end{bmatrix}, \\
 g(q) &= \begin{bmatrix} \theta_4 g \cos(q_1) + \theta_5 g \cos(q_1 + q_2) \\ \theta_5 g \cos(q_1 + q_2) \end{bmatrix}, \quad q = \begin{bmatrix} q_1 \\ q_2 \end{bmatrix}, \quad u = \begin{bmatrix} \tau \\ 0 \end{bmatrix}.
 \end{aligned}$$

and

$$\theta_1 = m_1 l_{c1}^2 + m_2 l_1^2 + I_1, \quad \theta_2 = m_2 l_{c2}^2 + I_2, \quad \theta_3 = m_2 l_1 l_{c2}, \quad \theta_4 = m_1 l_{c1} + m_2 l_1$$

$$\theta_5 = m_2 l_{c2}$$

m_1 : the total mass of link one

l_1 : the length of link one

l_{c1} : the distance to the center of mass of link 1

I_1 : the moment of inertia of link one about its centroid.

m_2 : the total mass of link two

l_{c2} : the distance to the center of mass of link two

I_2 : the moment of inertia of link two about its centroid

g : the acceleration due to gravity

The Pendubot parameters are $\theta_1 = 0.0308$, $\theta_2 = 0.016$, $\theta_3 = 0.0095$, $\theta_4 = 0.2087$ and $\theta_5 = .063$. The matrix $D(q)$ is invertible for all $q \in R^2$; hence, the state equations can be written as

$$\begin{aligned}\ddot{q} &= D^{-1}(q)[u - C(q, \dot{q})\dot{q} - g(q)] \\ x_1 &= q_1, x_2 = \dot{q}_1, x_3 = q_2, x_4 = \dot{q}_2 \\ \dot{x}_1 &= x_2 \\ \dot{x}_2 &= \ddot{q}_1 \\ \dot{x}_3 &= x_4 \\ \dot{x}_4 &= \ddot{q}_2.\end{aligned}$$

4.3 The Equilibrium Manifold

For each constant value of τ the Pendubot will have a continuum of equilibrium configurations. Since at equilibrium we $\ddot{q}_1 = \dot{q}_1 = \ddot{q}_2 = \dot{q}_2 = 0$, we have

$$\begin{aligned}\theta_4 \cos(q_1) + \theta_5 \cos(q_1 + q_2) &= \frac{\tau}{g} \\ \theta_5 \cos(q_1 + q_2) &= 0\end{aligned}$$

and the Pendubot will balance at

$$\begin{aligned}q_1 &= \cos^{-1}\left(\frac{\tau}{\theta_4 g}\right) \\ q_2 &= n\frac{\pi}{2} - q_1, \quad n = 1, 3.\end{aligned}$$

4.4 Controlling The Pendubot

The Pendubot control strategy developed for the Pendubot in [18], [5] is divided into two parts: a balancing control which balances the Pendubot about the desired equilibrium point, and a swinging control that swings the Pendubot up from the downward configuration to the desired configuration.

Balancing Control

The balancing problem may be solved by linearizing the equation of motion about an operating point using Taylor series expansion and designing a linear state feedback controller. As we saw before, the Pendubot has an equilibrium manifold which is a continuum of balancing positions. The linearized system becomes uncontrollable at $q_1 = 0, \pi$ as illustrated in Figure 4.2 which shows controllable and uncontrollable positions of the arm.

Swing Up Control

The problem of swinging the Pendubot up from the downward position to the inverted position is an interesting and challenging nonlinear control problem.

From the equation of motion we have

$$d_{11}\ddot{q}_1 + d_{12}\ddot{q}_2 + h_1 + \phi_1 = \tau \quad (4.2)$$

$$d_{21}\ddot{q}_1 + d_{22}\ddot{q}_2 + h_2 + \phi_2 = 0, \quad (4.3)$$

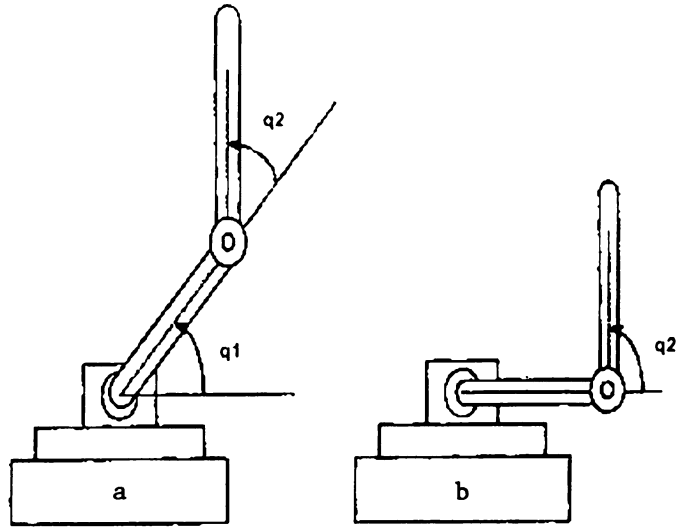


Figure 4.2. The pendubot arm at a: Controllable position, b: Uncontrollable position

where

$$D(q) = \begin{bmatrix} d_{11} & d_{12} \\ d_{21} & d_{22} \end{bmatrix},$$

$$C(q, \dot{q}) = \begin{bmatrix} h_1 \\ h_2 \end{bmatrix}, \quad g(q) = \begin{bmatrix} \phi_1 \\ \phi_2 \end{bmatrix}.$$

Solving for \ddot{q}_2 from (4.3) and substituting in (4.2), we obtain

$$\ddot{q}_1 \left(d_{11} - \frac{d_{12}d_{21}}{d_{22}} \right) + \left(h_1 - \frac{d_{12}h_2}{d_{22}} \right) + \left(\phi_1 - \frac{d_{12}\phi_2}{d_{22}} \right) = \tau.$$

Taking the control variable τ as

$$\tau = \left(d_{11} - \frac{d_{12}d_{21}}{d_{22}} \right) v_1 + \left(h_1 - \frac{d_{12}h_2}{d_{22}} \right) + \left(\phi_1 - \frac{d_{12}\phi_2}{d_{22}} \right)$$

results in

$$\left. \begin{aligned} \ddot{q}_1 &= v_1 \\ d_{22}\ddot{q}_2 + h_2 + \phi_2 &= -d_{21}v_1 \end{aligned} \right\}. \quad (4.4)$$

The control v_1 is taken as

$$v_1 = k_p(q_1^d - q_1) + k_d(\dot{q}_1^d - \dot{q}_1)$$

to track some reference positions $r = q_1^d, \dot{r} = \dot{q}_1^d = 0$ and the positive constants k_p and k_d are the control gains. Defining the tracking errors as

$$e_1 = q_1^d - q_1, \quad e_2 = \dot{q}_1^d - \dot{q}_1$$

$$\eta_1 = q_2, \quad \eta_2 = \dot{q}_2$$

the system (4.4) can be rewritten as

$$\dot{e}_1 = e_2$$

$$\dot{e}_2 = -k_p e_1 - k_d e_2$$

$$\begin{aligned}\dot{\eta}_1 &= \eta_2 \\ \dot{\eta}_2 &= -\frac{1}{d_{22}}(h_2 + \phi_2) - \frac{d_{12}}{d_{22}}k_p(q_1^d - q_1) + k_d(\dot{q}_1^d - \dot{q}_1) \\ y &= e_1.\end{aligned}$$

The tracking error part can be written as

$$\dot{e} = \begin{bmatrix} 0 & 1 \\ -k_p & -k_d \end{bmatrix} = Ee,$$

where $e = [e_1, e_2]^T$, k_p and k_d are chosen to make E Hurwitz. On the sliding surface $e = 0$, the dynamics are given by

$$\dot{\eta}_1 = \eta_2 \tag{4.5}$$

$$\dot{\eta}_2 = -\frac{1}{d_{22}}(h_2 + \phi_2) \tag{4.6}$$

which represents the zero dynamics with respect to the output $y = e_1$. We see from (4.5) and (4.6) that the zero dynamics are just the dynamics of the unactuated arm, which has a periodic orbit. While the error $e(t)$ converges to zero, the steady-state behavior for the first link converges exponentially to q_1^d and the second link oscillates about $(-\pi, 0)$. The swing up control job then is to excite the zero dynamics sufficiently by the motion of link 1 such that the pendulum swings close to its unstable equilibrium. When the pendulum is close to the desired equilibrium, the controller is switched from a partial feedback linearization controller to the linear balancing controller.

4.5 Hardware Description

The Pendubot consists of two rigid aluminum links of length 14 *in* and 8 *in*. Link one is directly coupled to the shaft of a 90 V permanent magnet DC motor mounted to the end of the table. The motor mount and bearing support the entire system. Link one includes the bearing housing for two joints. The shaft extends out in both directions of the housing, allowing coupling to the second link and to an optical encoder mounted on link one. The design gives both links full 360° of rotational motion. The optical encoders resolution is 1250 *pulse/rev*.

All the control computations are performed in Pentium PC with a D/A card and encoder interface card. Using the software routines supplied with the Pendubot, the control algorithm are programmed in C.

4.6 Observer design

As the optical encoders only measure the positions of the links, i.e., the angles q_1 and q_2 , we estimate the angular velocities \dot{q}_1 and \dot{q}_2 using a nonlinear high-gain observer

$$\dot{\hat{x}} = A\hat{x} + B\phi_0(\hat{x}, u) + H(y - C\hat{x})$$

where

$$\phi_0 = D^{-1}(q)[u - C(q, \dot{q})\dot{q} - g(q)]$$

and

$$A = \begin{bmatrix} 0 & 1 & 0 & 0 \\ 0 & 0 & 0 & 0 \\ 0 & 0 & 0 & 1 \\ 0 & 0 & 0 & 0 \end{bmatrix}, B = \begin{bmatrix} 0 & 0 \\ 1 & 0 \\ 0 & 0 \\ 0 & 1 \end{bmatrix},$$
$$C = \begin{bmatrix} 1 & 0 & 0 & 0 \\ 0 & 0 & 1 & 0 \end{bmatrix}, H^T = \begin{bmatrix} \frac{2}{\epsilon} & \frac{1}{\epsilon^2} & 0 & 0 \\ 0 & 0 & \frac{2}{\epsilon} & \frac{1}{\epsilon^2} \end{bmatrix}.$$

The observer parameter $\epsilon > 0$ was chosen to be .008, to recover the performance under state feedback.

4.7 Addition of Uncertainty

The Pendubot was stabilized at angles $q_1 = 75^\circ$ and $q_2 = 15^\circ$ using the control strategy developed for the Pendubot in Section 4.4, which applies first a swing-up control to swing the Pendubot from the downward configuration to its desired equilibrium position and then applies a balancing controller to do the balancing. A linear balancing controller

$$u = 16.4615(x_1 - 1.3090) + 3.1287x_2 + 16.242(x_3 - .2618) + 2.0658x_4 + 0.5296$$

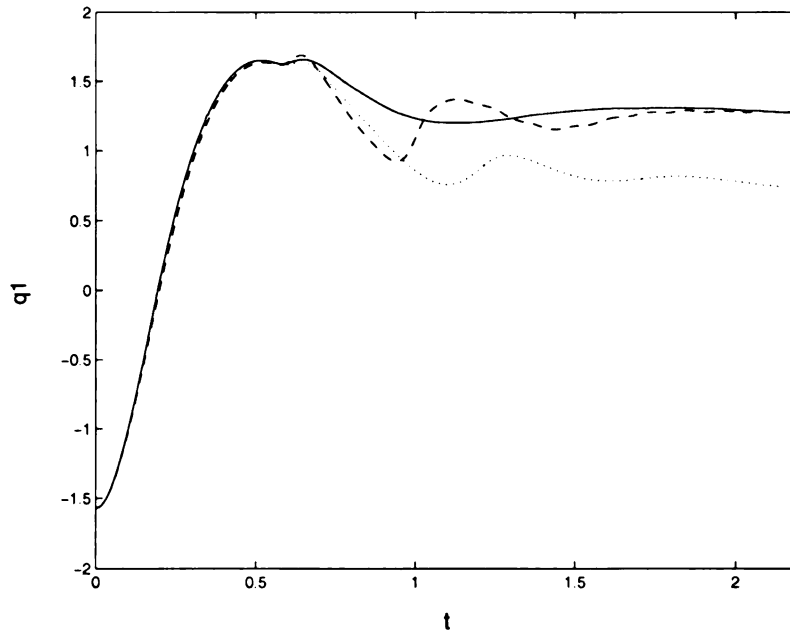


Figure 4.3. Trajectories for angle q_1 for different balancing controls, linear controller with no disturbance (solid), linear controller with constant disturbance of 1.6V in the control (dotted), linear state feedback integral controller with constant disturbance of 1.6V in the control (dashed)

with $x_1 = q_1, x_2 = \dot{q}_1, x_3 = q_2$ and $x_4 = \dot{q}_2$ was obtained using pole placement techniques and linearized nonlinear equations of the Pendubot from [3]. The details of the controller design is presented in Appendix A. The linear controller regulated the states to desired values as shown in Figure 4.3. Matched uncertainty in the form of a constant disturbance of 1.6 Volt was added to the control leading to an offset in the motor torque and shifting of the equilibrium point causing steady-state error as shown in Figure 4.3.

4.8 Integral action

Traditional integral action was introduced in the balancing controller by augmenting the states with integrators such that at the equilibrium point of the new augmented system the steady-state error is zero. The linear state feedback integral controller is given by

$$u = 51.5023(x_1 - 1.3090) + 8.602x_2 + 40.0770(x_3 - .2618) + 5.1840x_4 + 23.3882\bar{e},$$

where \bar{e} is the augmented state. The performance of this controller in the presence of constant disturbance in the motor torque can be seen in Figure 4.3. Although the integral controller regulates the states to desired values, the transient response becomes more oscillatory.

4.9 Conditional Integrators

Conditional integrators were introduced to both improve the transient response and also achieve zero steady-state error. As the linear controller designed above achieves exponential stability of the Pendubot in the absence of disturbances, Assumption 1 is satisfied with quadratic Lyapunov function $V(x)$ and quadratic positive definite function $W(x)$. With both Lyapunov function and state equation being known, Assumption 2 is satisfied with $L(x) = 1$. Finally, it can be verified from the linearized nonlinear equations of the Pendubot in [3] that Assumption 3 and 4 are also satisfied.

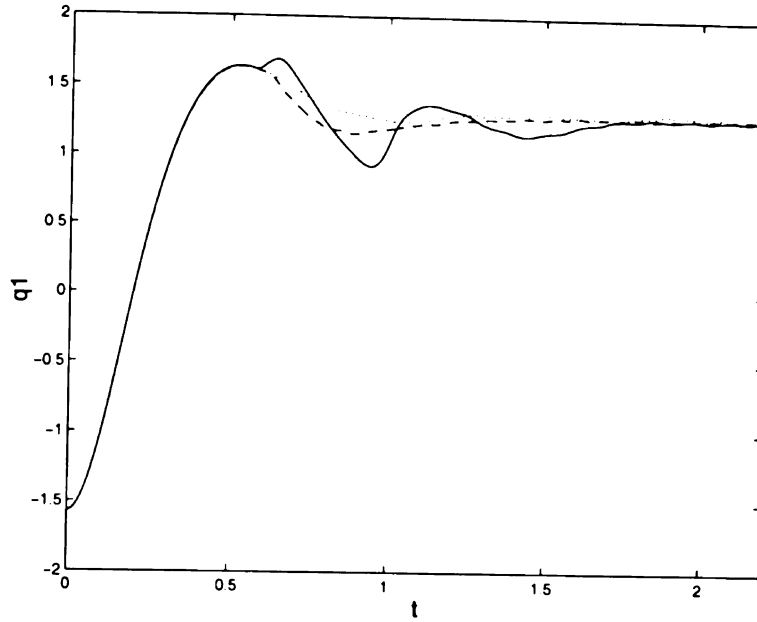


Figure 4.4. Trajectories for angles q_1 for different balancing controls with disturbance of 1.6V in the control, traditional integral action (solid), conditional integrator with $\mu=0.25$ (dashed), conditional integrator with $\mu=0.15$ (dotted)

The balancing controller is given by the saturated high-gain feedback

$$u = -3 \operatorname{sat} \left(\frac{y + \sigma}{\mu} \right)$$

$$y = 3.5[-.811(x_1 - 1.3090) - 0.145x_2 - .8045(x_3 - .2618) - 0.1x_4],$$

where the conditional integrator state σ is given by (7). As can be seen from Figure 4.4 and Figure 4.5, the controller achieves zero steady-state error and improves the transient response with decreasing μ . Note that the apparent discontinuity in the three figures corresponds to the point of switching from the swing-up controller to the balancing controller.

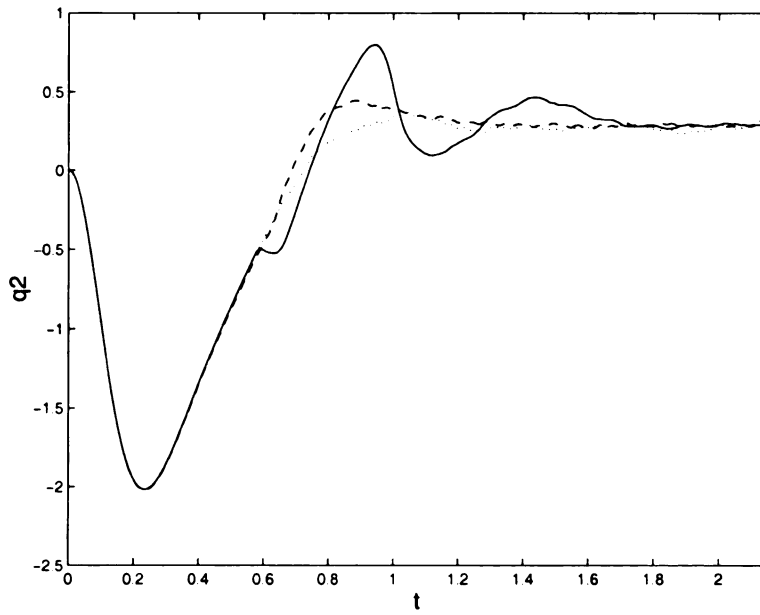


Figure 4.5. Trajectories for angles q_2 for different balancing controls with disturbance of $1.6V$ in the control, traditional integral action (solid), conditional integrator with $\mu=0.25$ (dashed), conditional integrator with $\mu=0.15$ (dotted)

CHAPTER 5

Conclusion

We presented conditional integrators as a tool for achieving asymptotic regulation of nonlinear systems subject to constant disturbances or parameter uncertainties, without compromising the transient response. We considered a fairly general class of nonlinear systems that can be stabilized by state feedback control and showed that, in the presence of matched parameter uncertainties that cause a shift in the equilibrium point, the system can be augmented with conditional integrators to recover asymptotic regulation of the state to the origin. We showed that the conditional integrator does not degrade the transient response, in the sense that as the width of a boundary layer approaches zero, trajectories of the system with conditional integrator approach those of a system with no integral action.

We also considered regulation of a class of minimum-phase, input-output linearizable, nonlinear systems where instead of regulating the states to the origin, they are regulated to a disturbance-dependent equilibrium point at which the regulation

error is zero. Output feedback control was implemented using high-gain observers. Towards the end, the performance of traditional and conditional integral control were demonstrated experimentally on the Pendubot. Asymptotic regulation with improved transient response was achieved with conditional integrators.

Appendix A

Controller Design

A.1 Linear Controller

The linearized nonlinear dynamic equation of the Pendubot about the operating point $q_1 = 75^\circ$ and $q_2 = 15^\circ$ is obtained from the Matlab code provided in [1]. The linearized equation is

$$\dot{\tilde{x}} = A\tilde{x} + B[u - 0.5296]$$

where $\tilde{x} = [x_1 - 1.3090, \dot{x}_1, x_2 - .2618, \dot{x}_2]^T$ and

$$A = \begin{bmatrix} 0 & 1 & 0 & 0 \\ 63.2865 & 0 & -23.8152 & 0 \\ 0 & 0 & 0 & 1 \\ -60.3877 & 0 & 102.9146 & 0 \end{bmatrix}, \quad B = \begin{bmatrix} 0 \\ 44.0722 \\ 0 \\ -82.6285 \end{bmatrix}. \quad (\text{A.1})$$

The controller gain matrix K was found using the *place* command of Matlab. The poles of the closed-loop system were placed at $-10.15 + 7.66i$, $-10.15 - 7.66i$, -8.3 and -4.2 .

A.2 Traditional Integral Action

Traditional integral action was introduced by augmenting the states with $\dot{e} = x_1 - 1.3090$. With the augmented state, the linearized equation is

$$\dot{\bar{x}} = A\bar{x} + B[u - 0.5296]$$

where $\bar{x} = [x_1 - 1.3090, \dot{x}_1, x_2 - .2618, \dot{x}_2, \bar{e}]^T$ and

$$A = \begin{bmatrix} 0 & 1 & 0 & 0 & 0 \\ 63.2865 & 0 & -23.8152 & 0 & 0 \\ 0 & 0 & 0 & 1 & 0 \\ -60.3877 & 0 & 102.9146 & 0 & 0 \\ 1 & 0 & 0 & 0 & 0 \end{bmatrix}, \quad B = \begin{bmatrix} 0 \\ 44.0722 \\ 0 \\ -82.6285 \\ 0 \end{bmatrix}.$$

The controller gains were found using the *place* command of Matlab. The poles of the closed-loop system were placed at -23.67 , $-6.76 + 5.1844i$, $-6.76 - 5.1844i$, -7.1618 and -4.88 .

A.3 Conditional Integrator

Let P be the solution of the Lyapunov equation

$$(A - BK)^T P + P(A - BK) = -Q,$$

where A, B are as given in (A.1), controller gain matrix K is chosen as in Appendix A.1 and the positive definite matrix Q is taken as

$$Q = \begin{bmatrix} .0206 & 0 & 0 & 0 \\ 0 & .0206 & 0 & 0 \\ 0 & 0 & .0206 & 0 \\ 0 & 0 & 0 & .0206 \end{bmatrix}.$$

Then, for the closed-loop system under the linear controller, Assumptions 1-4 are satisfied with

$$V(x) = x^T P x, \quad W(x) = -x^T Q x, \quad L(x) = 1, \quad h(x) = 2B^T P x$$

and control u is taken as (2.8).

BIBLIOGRAPHY

- [1] Pendubot Model P-2 User's Manual, Mechatronic System, Inc., Champaign, IL.
- [2] A.N. Atassi and H.K. Khalil. A separation principle for the stabilization of a class of nonlinear systems. *IEEE Trans. Automat. Contr.*, 44:1672–1687, 1999.
- [3] D.J. Block. Mechanical design and control of pendubot. Master's thesis, University of Illinois, Urbana Champaign , IL, 1991.
- [4] C.I. Byrnes, F.D. Priscoli, and A. Isidori. *Output Regulation of Uncertain Nonlinear Systems*. Birkhauser, Boston, 1997.
- [5] I. Fantoni, R. Lozano, and M.W. Spong. Energy based control of the pendubot. *IEEE Trans. Automat. Contr.*, 45:725–729, 2000.
- [6] K. Furuta and M. Yamakita. Swing up control of inverted pendulum. In *International Conference on Industrial Electronics, Control and Instrumentation*, Kobe, Japan, 1991.
- [7] J. Huang and W.J. Rugh. Stabilization on zero-error manifolds and the nonlinear servomechanism problem. *IEEE Trans. Automat. Contr.*, 37:1009–1013, 1992.
- [8] A. Isidori. *Nonlinear Control Systems*. Springer-Verlag, New York, 3rd edition, 1995.
- [9] A. Isidori and C.I. Byrnes. Output regulation of nonlinear systems. *IEEE Trans. Automat. Contr.*, 35(2):131–140, 1990.
- [10] H.K. Khalil. Universal integral controller for minimum phase nonlinear systems. *IEEE Trans. Automat. Contr.*, 45(3):490–494, 2000.
- [11] H.K. Khalil. *Nonlinear Systems*. Prentice Hall, Upper Saddle River, New Jersey, 3rd edition, 2002.

- [12] N.A. Mahmoud and H.K. Khalil. Asymptotic regulation of minimum phase nonlinear systems using output feedback. *IEEE Trans. Automat. Contr.*, 41:1402–1412, 1996.
- [13] L. Sciavicco and B. Siciliano. *Modeling and Control of Robot Manipulators*. McGraw-Hill, New York, 1996.
- [14] S. Seshagiri and H.K. Khalil. Robust output feedback regulation of minimum-phase nonlinear systems using conditional integrators. 2005. To appear in *Automatica*.
- [15] M. Spong. Energy based control of a class of underactuated mechanical systems. In *IFAC World Congress*, San Francisco, CA, 1996.
- [16] M. Spong and L. Praly. Control of underactuated mechanical systems using switching and saturation. In *Proc. of the Block Island Workshop on Control Using Logic Based Switching*, Springer-Verlag, 1996.
- [17] M. W. Spong and M. Vidyasagar. *Robot Dynamics and Control*. Wiley, New York, 1989.
- [18] M.W. Spong and D.J. Block. The Pendubot: A mechatronic system for control research and education. In *Proc. IEEE Conf. on Decision and Control*, pages 555–556, New Orleans, LA, 1995.

MICHIGAN STATE UNIVERSITY LIBRARIES



3 1293 02504 2957